TECHNICAL MEMORANDUM

NASA TM X-3314

AND PRELIMINARY TESTS OF A BLADE TIP SS INJECTION SYSTEM FOR VORTEX CATION AND POSSIBLE NOISE REDUCTION ULL-SCALE HELICOPTER ROTOR

Pegg, Robert N. Hosier, Balcerak, and H. Kevin Johnson

Research Center Va. 23665

RONAUTICS AND SPACE ADMINISTRATION • WASHINGTON, D. C. • DECEMBER 1975

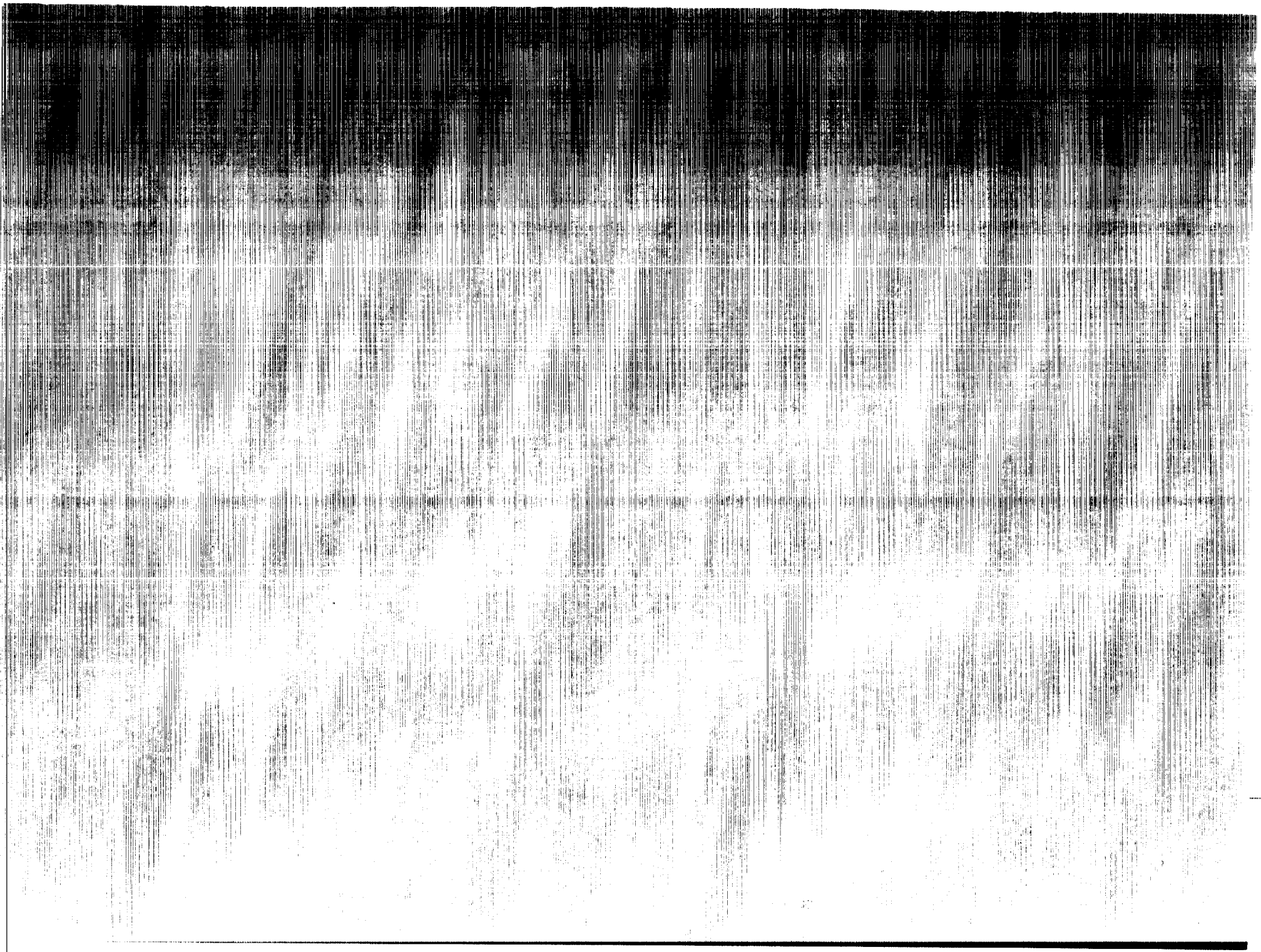

1. Report No. NASA TM X-3314	2. Government Accession No.	3. Recipient's Catalog No.
4. Title and Subtitle DESIGN AND PRELIMINARY TESTS OF A BLADE TIP AIR MASS INJECTION SYSTEM FOR VORTEX MODIFICATION AND POSSIBLE NOISE REDUCTION ON A FULL-SCALE HELICOPTER ROTOR		5. Report Date December 1975 6. Performing Organization Code
7. Author(s) Robert J. Pegg, Robert N. Hosier, John C. Balcerak, and H. Kevin Johnson		8. Performing Organization Report No. L-10428 10. Work Unit No. 505-10-26-02
9. Performing Organization Name and Address NASA Langley Research Center Hampton, Va. 23665		11. Contract or Grant No. 13. Type of Report and Period Covered Technical Memorandum
12. Sponsoring Agency Name and Address National Aeronautics and Space Administration Washington, D.C. 20546		14. Sponsoring Agency Code

15. Supplementary Notes

Robert J. Pegg: Langley Research Center.

Robert N. Hosier: Langley Directorate, U.S. Army Air Mobility R&D Laboratory.

John C. Balcerak and H. Kevin Johnson: Rochester Applied Science Associates Division, Systems Research Laboratories, Inc., Rochester, New York.

16. Abstract

Full-scale tests were conducted on the Langley helicopter rotor test facility as part of a study to evaluate the effectiveness of a turbulent blade tip air mass injection system in alleviating the impulsive noise (blade slap) caused by blade-vortex interaction. Although blade-slap conditions could not be induced during these tests, qualitative results from flow visualization studies using smoke showed that the differential velocity between the jet velocity and the rotor tip speed was a primary parameter controlling the vortex modification.

17. Key Words (Suggested by Author(s))	18. Distribution Statement
Acoustics Helicopter rotor Tip jet Vortex modification	Unclassified – Unlimited Subject Category 01

19. Security Classif. (of this report)	20. Security Classif. (of this page)	21. No. of Pages	22. Price*
Unclassified	Unclassified	38	$3.75

*For sale by the National Technical Information Service, Springfield, Virginia 22161

DESIGN AND PRELIMINARY TESTS OF A BLADE TIP AIR MASS INJECTION SYSTEM FOR VORTEX MODIFICATION AND POSSIBLE NOISE REDUCTION ON A FULL-SCALE HELICOPTER ROTOR

Robert J. Pegg, Robert N. Hosier,* John C. Balcerak,**
and H. Kevin Johnson**
Langley Research Center

SUMMARY

Full-scale tests were conducted on the Langley helicopter rotor test facility (HRTF) as part of a study to evaluate the effectiveness of a turbulent blade tip air mass injection (TAMI) system in alleviating the impulsive noise (blade slap) caused by blade-vortex interaction. Although blade-slap conditions could not be induced during these tests, qualitative results from flow visualization studies using smoke showed that the differential velocity between the jet velocity and the rotor tip speed was a primary parameter controlling the vortex modification. The vortex cores which were injected at high differential velocities were consistently larger than either the cores of noninjected vortices or the cores of vortices injected at low differential velocities. Rotor noise prediction based on observed aerodynamic data has indicated the possibility of substantial noise reduction as a result of the application of the TAMI system. The experimental acoustic data indicate that wind-tunnel or flight tests would be required to quantify the predicted changes in noise levels caused by the restructuring of the blade tip vortices in blade-slap conditions.

INTRODUCTION

When a rotor develops lift, a vortex is formed at the blade tip. This vortex consists of a finite core of viscous fluid rotating as a solid body and an extended annular region of rotational motion characterized by the absence of vorticity. The finite core is of immediate concern to rotary wing dynamicists, aerodynamicists, and acousticians because of the detrimental effects that can occur when the core interacts with a lifting surface. These include increased oscillating blade loads and high levels of impulsive noise which can be the dominant rotor noise when it occurs.

---

*Langley Directorate, U.S. Army Air Mobility R&D Laboratory.
**Rochester Applied Science Associates Division, Systems Research Laboratories, Inc., Rochester, New York.

The characteristics of the vortex flow field and the associated pressure pulses created by its interaction with a rotor blade have been investigated by various theoretical and experimental methods (refs. 1 to 6). The consensus of these investigations is that the mechanism for impulsive noise caused by blade-vortex interations (blade slap) is a large-amplitude pressure pulse occurring on a rotor blade section over a short period of time. This incremental loading is caused by the induced velocity field of the vortex which forces a rapid change in the blade section angle of attack. The magnitude of this angle-of-attack change is directly proportional to the strength of the vortex and inversely proportional to the spacing between the vortex and the blade section. Other parameters fundamental to the blade-slap phenomenon are the time increment over which the blade-vortex interaction occurs, the orientation of the vortex with respect to the blade, and the blade span over which the interaction occurs.

A system to modify the tip vortex and minimize interaction effects would be a great benefit acoustically. An ideal system would not allow the vortex to reform, while an acceptable system would not allow the vortex to reform within at least three rotor revolutions in order to miss the following blades. Also, any system should have a minimal effect on rotor performance. Many active and passive blade tip modifications have been tried, but none have shown both significant noise reduction and low performance penalties. However, recent wind-tunnel tests (refs. 3 and 4) of a nonrotating blade tip air mass injection (TAMI) system have shown that the initial spreading of the trailed tip vortex continued with time in accordance with Lamb's viscous model (ref. 7) and with no apparent vortex reformation for at least three equivalent rotor revolutions. In addition, only a small performance degradation was observed. In order for the TAMI system to work efficiently, two factors were found to be critical: (1) The geometric alinement of the injection jet axis with the tip vortex core and (2) the differential velocity between that of the tip jet and the free stream at the blade tip.

Because of the promise of the nonrotating TAMI wind-tunnel tests, a research program was conducted on the Langley helicopter rotor test facility (HRTF) to determine the effects of TAMI on the acoustic signature and performance characteristics of a full-scale, rotating, helicopter rotor system. In addition, these test data were used in conjunction with nonrotating full- and reduced-scale wind-tunnel data to predict the acoustic and performance benefits of the TAMI system. This paper reports the results of experimental and predictive efforts.

SYMBOLS

A cross-sectional area of jet nozzle, m

a speed of sound, m/sec

c	chord of blade, m
h	blade-vortex spacing, m
$\dot{m}$	mass flow rate, kg/sec
p_o	reference pressure, dynes/cm^2
$r_{c,i}$	radius of injected vortex core, m
$r_{c,o}$	radius of noninjected vortex core, m
T_j	tip jet thrust, N
T_r	rotor thrust, N
V_j	tip jet velocity, m/sec
V_t	rotor tip velocity, m/sec
$V_{\theta,i}$	tangential velocity of injected vortex core, m/sec
$V_{\theta,o}$	tangential velocity of noninjected vortex core, m/sec
V_∞	free-stream velocity, m/sec
α	angle of attack of lifting surface, deg
Γ_o	lifting-surface circulation, m^2/sec
ρ	air density, kg/m^3
Ω	rotor rotational speed, rpm

Abbreviations:

BW	bandwidth
SPL	sound pressure level

BLADE TIP AIR MASS INJECTION (TAMI)

Test Program

Impulsive noise from rotor systems primarily occurs under two different conditions. The first is associated with high-speed flight when the blade operates periodically in the compressible-flow region and the compression shocks create an unsteady blade loading which, in turn, generates an impulsive noise. Also, monopole thickness effects become extremely important at high tip Mach numbers. The second condition is assoicated with blade-vortex interactions where a large-amplitude pressure pulse occurs on a rotor blade section over a short period of time. This incremental loading is caused by the induced velocity field of the vortex which forces a rapid change in the angle of attack at the blade section. In this case, the magnitude of the angle-of-attack change is directly proportional to the strength of the vortex and inversely proportional to the spacing between the vortex and blade section. The term "blade slap" is used to describe the noise caused by blade-vortex interaction.

TAMI or any vortex modification system would be ineffective in alleviating noise caused by the first condition. For the second condition, TAMI would be expected to be effective because it reduces the peak tangential velocity of the vortex. This reduction in the peak tangential velocity may alleviate blade-slap noise by reducing the magnitude of the peak pressure pulse, by increasing the duration of the pressure pulse, or by preventing a blade section from entering a local compressible-flow region.

Impulsive Noise (Blade Slap) Criteria in Hover

Recent research efforts (ref. 8) indicate that the blade-vortex interactions can occur over a wide range of hover operating conditions. It was found that both slapping and non-slapping conditions had blade-vortex interactions, however, so this interaction could not completely account for the impulsive noise; it was concluded that if a lightly loaded blade, operating at a low tip speed, interacted with a weak vortex, the impulsive noise would not occur. It was also hypothesized that blade-vortex interactions could generate impulsive noise depending on the local operating parameters at the points of interaction. The criterion, based on subjective evaluation and flow visualization analysis, seemed to be that impuslive noise would occur in hover if the critical Mach number were reached or exceeded at the rotor section when blade-vortex interactions occurred.

Based on these previous experimental and theoretical results, a UH-1D rotor system was modified and tested on the HRTF. A description of the rotor system modifications and test conditions follows.

Description of Rotor System Modifications

Two UH-1D rotor blades were used in the test program. The blades had a modified NACA 0012 airfoil section, a 0.533-m chord, a 7.314-m radius, and a linear twist of -10.8°. The rotor system was installed on the HRTF using a standard UH-1 rotor hub assembly.

The blades were modified to provide an air supply to the blade tips by using the D-spar as part of the system. The cover plate over the D-spar at the root was modified to accept a 0.0318-m-diameter elbow for the supply of air from the source through a rotating union. (See fig. 1.) The air injection system at the tips of the rotor blades was contained in 0.0389-m extensions to each of the blades, and outboard of these extensions the tips of the blades were contoured to the basic airfoil coordinates to produce "half-round" airfoil tips. Contained within the extensions were the nozzles for TAMI. The tip extension (fig. 2) consisted of two principal parts: a D-spar cap and a nozzle fairing. The nozzle fairing was contoured from balsa. A 0.0343-m hole was drilled through the balsa at a 6° angle so that the center line of the hole exited at the three-quarter chord of the upper surface of the airfoil. The balsa section was bonded to the existing end rib of the rotor blade, and a fiberglass skin was bonded over the balsa tip and outer section of the rotor blade. The tubular nozzles were fitted snugly into the hole in the balsa and were cut along the contour of the airfoil section (fig. 3). The nozzles were held in place in the chordwise direction by a set screw.

The air supply line to the rotor blades was suspended above the rotor system on the HRTF where it attached to the fixed end of a rotary union (fig. 1). The rotating end of the union was attached to the upper mast head and had two discharge ports so that air was channeled into the base of each D-spar through a short contour hose.

The deflection and stresses of the D-spar imposed by the internal pressurization of the structure were determined experimentally. A maximum stress of approximately 50 kN/m^2 was measured at an internal pressure of 0.38 kN/m^2. This stress was within the limit set by the rotor blade manufacturer.

Description of Instrumentation

The HRTF test program consisted of five test series; the rotor system and HRTF instrumentation varied among the tests. The rotor blade was initially instrumented with pressure transducers and strain gages to record vortex interactions. These transducers became inoperative early in the test program; consequently, no pressure data were obtained.

Acoustic instrumentation.- As listed in table I, eight ground-positioned microphones were used in the first test series to measure the rotor noise. In the second and fifth test

series, six ground-positioned microphones were used, while one microphone was positioned upwind in the plane of the rotor system and another microphone was positioned on axis 4.57 m above the rotor system. Figure 4 shows the positions of the microphones for test series 5. The position 46 m from the shaft axis (test series 1) resulted in an inclination angle of approximately 10^{o}. In the second and fifth test series, the microphones were placed a greater distance from the rotor and closer to the ground than in the first series to lower the broadband noise signature relative to the rotational noise signal and to move the ground interference effects to higher frequencies.

All microphones were fitted with windscreens and were oriented for grazing incidence. The microphones were commercially available and were of a piezoelectric, ceramic type having a flat frequency response to within 3 dB from 20 Hz to 12 000 Hz. The signal outputs from all microphones were recorded on multichannel, frequency-modulated magnetic tape recorders at 152.4 cm/sec with a center frequency of 108 kHz.

The entire sound measurement system was calibrated in the field prior to and after each day's testing by means of conventional discrete frequency calibrators with a 1000-Hz sine-wave signal at a sound pressure level of 114 dB. Real-time correlation between all microphone positions was recorded on magnetic tape with a standard IRIG format B time code. Data records were analyzed to obtain sound-pressure-level time histories and spectra data. All measurements were made with a reference value of 20 $\mu N/m^2$ in accordance with recommendations of reference 9 and have not been corrected for atmospheric effects.

Flow visualization equipment.- A smoke-generating rake was positioned slightly above the rotor plane so that the smoke flow would be pulled down through the rotor. A 16-mm high-speed camera was used to photograph the trajectories of the resulting tip vortices.

Rotor performance instrumentation.- Rotor performance parameters (thrust, torque, and rotational speed) were measured by the HRTF data acquistion system. This system, described in detail in reference 10, allows measurement of thrust, torque, blade pitch, and rotational speed within ±1 percent.

HRTF Tests

The conditions for each test series are listed in table II. In the first series, attempts were made to establish the conditions for which blade slap could be detected acoustically. TAMI was not used during this test series. The attempt was generally unsuccessful since only intermittent "spikes" in the acoustic signatures were noted. These spikes were believed to be associated with blade-vortex proximity but were not consistent enough to demonstrate blade-vortex interaction.

In addition, the flow visualization showed no change in the vortex core structure. The reason for this was believed to be a result of the speed differential between the jet and the tip speed of the rotor being too small. For example, at Ω = 320 rpm the tip speed of the rotor was approximately 245 m/sec, while at a jet thrust of 71 N and 142 N, the injection velocities were approximately 245 m/sec and 320 m/sec, respectively.

Because previous studies (e.g., ref. 3) had shown that the effects of TAMI were more pronounced as the velocity differential between the jet and the free stream was increased, convergent-divergent nozzles were fabricated to provide exit velocities of approximately 1.5 times the sonic velocity. Flow visualization tests were then conducted with TAMI applied to just one blade. These tests showed that the injected tip vortices consistently had a larger vortex core (and, thus, lower core velocities) as indicated by the absence of smoke over a larger area in the center of the vortex; also, the injected vortices diffused more quickly than the noninjected vortices, as indicated by the earlier breakup of the swirling pattern of the smoke.

RESULTS AND DISCUSSION OF TAMI TEST PROGRAM

It is obvious from the previous discussion of the HRTF tests that blade slap was not induced. To explain this result, the HRTF performance and flow visualization data were examined and compared with earlier results. A discussion of these results follows.

Effect of Rotor Thrust and Tip Speed on Blade Slap

Reference 8 shows that blade slap becomes more intense with increasing rotor thrust and tip speed. An approximate boundary where blade slap becomes dominant for many rotors is shown by the curve in figure 5 (fig. 13 of ref. 11). Also shown in figure 5 are the average span loadings for the highest thrust levels achieved during the HRTF tests at Ω = 250, 292, and 324 rpm. They indicate that the rotor thrust at Ω = 292 and 324 rpm were slightly below the loading levels where blade slap should be expected.

Effect of TAMI on Tip Vortex Dissipation and Rotor Performance

The flow visualization, performance, and acoustic data were analyzed to determine the characteristics of the rotor with and without TAMI. Changes in the wake parameters (core diameter and location) based on the flow visualization photographs were compared with previously measured changes in wake structure due to TAMI (refs. 3 and 4). The results are presented in the following sections.

Smoke visualization data.- The flow visualization data with TAMI from only one blade were analyzed to determine the trajectory of the trailed vortices and to determine whether any changes could be detected in vortex structure. With TAMI from one blade,

alternating injected and noninjected vortices were visualized. As can be seen in figure 6, the vortices are rather well defined by the smoke. The smoke is entrained in the vortex, but not in the vortex core. Therefore, the dark area in the center of the vortex generally defines the core size. It was noted from photographs like figure 6 (and substantiated by the results of ref. 3) that the differential velocity $V_j - V_t$ of the first test series was insufficient to cause a difference between injected and noninjected vortex cores.

Typical smoke flow visualization data from tests using the convergent-divergent nozzles (test series 4) are shown in figure 7. Again there was injection from one blade only. This time the injected core size increased noticeably in comparison to the non-injected cores. Measurements of the core diameters indicated that the injected cores were nearly four times larger than the noninjected cores. Reviews of high-speed movies also showed that the trailed vortices were convected downward and were not swept into the rotor plane for any of the conditions tested. Thus, no blade-vortex interaction occurred.

The fact that under identical blade operating conditions an injected vortex increased in size rapidly with a resultant decrease in its peak tangential velocity has been documented quantitatively (ref. 5). A critical parameter in the injection process has been found to be the nondimensional thrust parameter $T_j/\rho\Gamma_o{}^2$, where $T_j = \rho A(V_j - V_\infty)^2$. Experimental thrust parameter data from reference 5 and this program are shown in figures 8 and 9. For the nominal rotational speed of the UH-1D rotor, the core radius was nearly doubled for vortices injected at sonic velocities relative to the blade with a nondimensional thrust of approximately 0.01. Injection at about 1.5 times the sonic velocity, however, increased the nondimensional thrust parameter to the range $0.02 \leqq \frac{T_j}{\rho\Gamma_o{}^2} \leqq 0.07$ for the values of the rotor thrust tested. In these cases, an even larger change in vortex structure was observed in the smoke flow data as would be expected from figures 8 and 9.

The model data in figure 9 also show that the peak tangential velocity was decreased to a greater extent for the UH-1D blade section model than for a previously tested NACA 0015 wind-tunnel model with a 0.0203-m chord. This was attributed to the fact that the peaks of the turbulence spectra for the 1.27- to 1.59-cm sonic jets were in the same frequency range as the natural decay frequency of the unmodified vortex of the UH-1D model, whereas such frequency correlation did not exist for the NACA 0015 section model. This suggests that a close coupling between the turbulence spectrum of the jet and the swirling vortex may increase the effectiveness of TAMI.

The cores of the injected vortices were clearly distinguished by long smoke streamers extending downstream from the blades. Short streamers extended intermittently from the blades with the noninjected vortices. The long streamers are evidence that considerable mixing exists between the turbulent jet and the tangential flow of the vortex. This

turbulent mixing of two flows is the mechanism by which rapid vortex aging is accomplished. Without TAMI, only short streamers can be seen because of the limited mixing between the axial and tangential flows in the vortex.

Figures 10 and 11 (figs. 11 and 13 of ref. 5) show the measured tangential and differential axial velocity distributions of noninjected and injected vortices, respectively, for a nonrotating UH-1D blade section. The data for the noninjected vortex shows that the axial velocity is equal to the free-stream velocity 6.5 chord lengths downstream of the model.

Performance data.- The performance parameters measured during the HRTF tests were the rotor rotational speed, thrust, and torque. Although these data were recorded when the acoustic data were recorded, they were averaged over a longer time period. A summary of the performance data is shown in table III. The first entry in each block is that for the uninjected conditions, while succeeding entries are for the injected configurations.

The slight differences in the rotor thrust between the noninjected and injected configurations are believed caused by unsteadiness in the test conditions rather than by the effects of the jet. Previous investigations (refs. 3, 4, and 5) of the TAMI system in a fixed-wing wind-tunnel test also showed that the jet had practically no influence on the lifting or moment characteristics of the generating airfoil.

Table III presents the experimental performance data obtained from the rotor using the TAMI on the HRTF. The test conditions ranged from rotor thrust levels of 11.8 kN to 45.2 kN and power levels of 114.8 kW to 698.0 kW. Power to produce the maximum jet thrust levels was 47.7 kW, which is approximately 7 percent of the maximum full-scale rotor system power. This level was exclusive of pressure line losses.

Acoustic data.- A typical rotor noise spectrum from microphone position 4 at $T_r = 35.5$ kN and $\Omega = 324$ rpm is shown in figure 12. The spectrum shows that the rotational noise levels remain relatively constant from 150 to 350 Hz before falling off. The slight increase in noise levels above 150 Hz was attributed to variations of the wake vortices caused by random changes in the wind velocity during the test.

Analysis of the acoustic-pressure time history also showed the typical rotational noise characteristics with no evidence of a strong secondary peak, indicative of an induced pressure pulse caused by the proximity of a vortex. The sound pressure levels were also not at a level which could be considered indicative of blade slap.

An important consideration in the TAMI system is the effect of the noise of the rotor blade tip jet on the overall acoustic output of the rotor. The noise produced by one supersonic jet with an exit velocity of approximately 430 m/sec was measured at several different locations and rotor operating conditions so that the effect of motion on the jet noise could be defined. Figure 13(a) shows a spectrum of the jet noise recorded at the on-axis

microphone (position 8) with the blade held stationary and with the blade rotating under the jet thrust. The analysis bandwidth is 60 Hz and the spectrum is averaged over a record length of approximately 13 sec. As can be seen the level and shape of the spectrum for the stationary jet changed little when the jet was allowed to drive the rotor system. The rotor speed for this condition was 92 rpm, with V_t = 70 m/sec. The on-axis jet noise was calculated by using the procedure for supersonic jets outlined in reference 12. A spectrum peak frequency of 3.47 kHz was calculated, based on a Strouhal number of 0.2. In figure 13(b), the measured spectrum levels for $\Omega = 0$ in figure 13(a) have been corrected to BW = 1 Hz and compared with the calculated spectrum levels. The measured and calculated spectra show excellent agreement through 10 kHz. The differences seen above 10 kHz are believed to be caused by atmospheric absorption.

Figure 14 shows the on-axis noise produced by the rotor at 324 rpm and a rotor thrust of approximately 35.5 kN with and without TAMI. The on-axis jet noise caused by TAMI dominates the standard rotor noise from 2 kHz. Therefore, the on-axis frequency distribution of the jet noise is not strongly affected by blade rotation in the range $0 \leqq \Omega \leqq 324$ rpm.

Once the observer is located off the rotor axis, however, the effects of blade rotation become very important to the radiated jet noise. The circular motion of the jet complicates the emission pattern considerably, because the jet orientation and velocity (and acoustic directivity) are continually changing with respect to the observer. Figure 15 shows the radiated jet noise at the upwind, ground-microphone position when the jet drives the rotor system at 92 rpm. The analysis bandwidth was still 60 Hz. The peak jet noise for this condition was 64 dB at 2.7 kHz. The peak frequency is lower here than in figure 13 because the relative velocity has been reduced.

Figure 16 shows a comparison of the total noise output of the rotor system measured at microphone position 4 with and without TAMI (Ω = 324 rpm and T_r = 35.5 kN). The bandwidth of this analysis is 15 Hz and the spectrum is averaged over approximately 26 sec of the data sample. Figure 16 also shows that the jet noise is not observable at frequencies less than about 2.5 kHz. Above the 2.5 kHz, the rotor noise with TAMI on exceeds the standard rotor noise by approximately 4 dB but maintains the same spectral shape as the noninjected rotor. The tip jet noise would thus not be expected to be a problem in relation to annoyance or detection under standard rotor operating conditions.

PREDICTED EFFECT OF TAMI ON IMPULSIVE NOISE

This section describes first the predicted effect of blade-vortex spacing on rotor impulsive noise and then the predicted effect of TAMI on the impulsive noise by using

measured TAMI data from this and other experiments where possible and by assuming various values for the blade-vortex interaction parameters.

Effect of Mean Vortex Position and Size on Blade Slap

Figure 17 (from ref. 1) shows the effect of mean blade-vortex spacing on rotor impulsive noise. The measured and predicted sound pressure levels increase with decreasing h up to the point where h becomes less than a vortex core diameter. For smaller values of h the sound pressure levels remain nearly invariant. Figure 17 also shows the effect of core size on the rotor impulsive noise. As the core size is increased, a substantial decrease in sound pressure level is observed when compared to the noise levels from the basic core.

As discussed in reference 1, the time increment over which the blade-vortex interaction occurs, the orientation of the vortex with respect to the blade, and the blade span over which the interaction occurs also affect the levels of the impulsive noise. For example, if the core axis were normal to the blade radius and h were relatively constant over the interaction azimuth, the blade would be near the vortex for a relatively long time. However, if the core axis were parallel to the blade radius, the blade would be near the vortex for a relatively short time and would interact along a more extensive blade span. Assuming all the other vortex characteristics were similar, the latter type of blade-vortex interaction would be expected to produce significantly greater impulsive noise than the former type of interaction.

Description of Prediction Technique

The prediction technique was developed and verified in references 13 to 15. In performing the calculations presented in this report, the rotor aerodynamics were first assumed to be defined by a uniform inflow velocity. This uniform inflow velocity was then modified by the induced effects of a trailing tip vortex. The induced effects of the tip vortex were calculated for several positions below the rotor plane. The mean vertical position of the vortex core axis was assumed to be normal to the blade and a uniform distance of 0.854 m below the rotor as measured from the HRTF flow visualization data. The vertical position of the vortex was then varied sinusoidally about the mean position of 0.854 m. A sinusoidal variation was chosen because of the variations in vortex positions described in the whirl tower tests of reference 8. The minimum separation distances between the axis of the vortex core and the blade were arbitrarily chosen to be 0.025, 0.104, 0.153, and 0.305 m. The distance of 0.025 m corresponds to approximately one core radius of the uninjected vortex. The observer location for the noise prediction corresponded to microphone position 4. The effects of broadband noise were not included in the analyses.

Impulsive Noise Predictions for Vertical Sinusoidal Vortex Displacements Based on HRTF Data

The calculated pressure time histories of the rotor noise for minimum separation distances of 0.305, 0.153, and 0.025 m are shown in figure 18. The pressure time history for the 0.305-m separation (fig. 18(a)) is approximately what would be expected for classical rotational noise (fig. 17). As the vortex approaches the blade it begins to introduce a spike in the pressure trace. Figure 18(b) shows the beginning of such a spike for a minimum separation distance of 0.153 m. The peak-to-peak pressure has increased from 94 dynes/cm^2 for a separation distance of 0.305 m to 159 dynes/cm^2 for a separation distance of 0.153 m; however, the wave form is not nearly as pronounced as the one introduced at 0.025 m (fig. 18(c)). In this case, the spike has caused the peak-to-peak pressure to increase 775 dynes/cm^2 and become much shorter in duration. This separation distance models blade slap quite well.

The predicted acoustic spectra for a vertical sinusoidal vortex with minimum blade-vortex separation distances of 0.305, 0.153, and 0.025 m are shown in figure 19. The spectra have a bandwidth of 1.5 Hz. The predicted spectrum for a separation distance of 0.305 m (fig. 19(a)) compares quite well with the measured spectrum (fig. 12) in the frequency range of 0 to 150 Hz. At frequencies higher than 150 Hz, however, the predicted noise is significantly lower than the measured noise. When the minimum separation distance is decreased (while maintaining the same mean position), the spectral harmonic content is increased and, as would be expected, agreement with the HRTF measured rotational noise spectrum is poor. This is shown in the predicted spectrum of figure 19(b) for a minimum separation distance of 0.025 m.

The last set of conditions listed in table III was not tested; the tests, however, show that the supersonic nozzle that was installed for the HRTF tests was sufficient to reduce the peak tangential velocity in the tip vortex by approximately 50 percent, even for a relatively high loading condition. The decrease in the peak tangential velocities would be expected to have a pronounced effect on the local induced velocity at a blade section. This can be related to the core size, since it can be realistically assumed that a vortex will approach a blade only to within its core radius. In this representation, the total circulation of the vortex remains invariant with respect to the size of the core.

The data in figure 10 show that the core of the injected vortex would be expanded by a factor of 4, so that the axis of the vortex core could approach the blade to within 0.104 m. The noise spectrum for this condition under the same assumptions used for the noise predictions discussed earlier is shown in figure 20. Comparison of this spectrum with that of the nonexpanded core (fig. 19(c)) shows a drop in noise level of 8 dB at 100 Hz, 14 dB at 200 Hz, 25 dB at 300 Hz, 20 dB at 400 Hz, and 10 dB at 500 Hz. This reduction in radiated noise is substantial, especially when the subjective aspects are considered. The predicted

noise level seems to be realistic in view of the substantial differences in the measured peak tangential velocities.

For all wake conditions, the noise predictions below 50 Hz were insensitive to the wake effects and show excellent agreement with the measured rotational noise. This analysis shows that the rotational noise of the rotor can be well predicted if the wake parameters can be defined in sufficient detail. It also verifies the higher harmonic sensitivity to vortex position previously noted in the experimental spectrum.

CONCLUDING REMARKS

Full-scale rotor tests were conducted on the Langley helicopter rotor test facility (HRTF) to evaluate the effectiveness of a turbulent tip air mass injection (TAMI) system in alleviating the impulsive noise (blade slap) caused by blade-vortex interaction. Although blade-vortex interaction conditions could not be induced during these tests, qualitative results from flow visualization of the tip vortices using smoke showed that the differential velocity between the injected jet and rotor tip speed was a primary parameter controlling the results of the injection process. The final TAMI configuration used a convergent-divergent nozzle at the blade tip. High-speed flow visualization of the shed vortices indicated that considerable mixing occurs between the injected jet flow and the swirl flow about these vortices. The minimum value of the nondimensional thrust parameter was approximately 0.02. This supports nonrotating wind-tunnel tests.

Measured acoustic data concerning the tip jet noise indicated that this source of noise was negligible in comparison to the typical noise produced by the rotor system. Based on measurements of the jet flow it is estimated that the TAMI system requires approximately 7 percent of the measured maximum full-scale rotor system power. Acoustic predictions of the rotor noise, using the TAMI experimental data obtained during these tests, show that at inflight conditions, where blade-vortex interactions are expected to occur, the sound pressure levels of the harmonics between 100 and 500 Hz may be reduced as much as 25 dB.

Langley Research Center
National Aeronautics and Space Administration
Hampton, Va. 23665
November 10, 1975

REFERENCES

1. Widnall, Shelia; Chu, Sing; and Lee, Albert: Theoretical and Experimental Studies of Helicopter Noise Due to Blade-Vortex Interaction. Helicopter Noise Symposium, U.S. Army Res. Office – Durham and American Helicopter Soc., Inc., Sept. 1971, pp. 25-34.

2. Padakannaya, Raghuveera: The Vortex Lattice Method for the Rotor-Vortex Interaction Problem. NASA CR-2421, 1974.

3. Balcerak, John C.; and Feller, Raymond F.: Vortex Modification by Mass Injection and by Tip Geometry Variation. USAAMRDL Tech. Rep. 73-45, U.S. Army, June 1973. (Available from DDC as AD 771 966.)

4. Balcerak, John C.; and Zalay, Andrew D.: Investigation of the Effects of Mass Injection To Restructure a Trailing Tip Vortex at Transonic Speeds. Rep. 73-03 (Contract No. N00014-71-C-0226), Rochester Appl. Sci. Assoc., Inc., Feb. 1973. (Available from DDC as AD 760 363.)

5. Zalay, Andrew D.; White, Richard P.; and Balcerak, John C.: Investigation of Viscous Line Vortices With and Without the Injection of Core Turbulence. Rep. 74-01 (Contract No. N00014-71-C-0226), Rochester Appl. Sci. Assoc., Inc., Feb. 1974. (Available from DDC as AD 785 256.)

6. White, Richard P., Jr.; Balcerak, John C.; and Pegg, Robert J.: Summary of Results Indicating the Beneficial Effects of Rotor Vortex Modification. Proceedings of National Symposium on Helicopter Aerodynamic Efficiency, American Helicopter Soc., Inc., Mar. 1975, pp. 5-1 – 5-15.

7. Lamb, Horace: Hydrodynamics. Sixth ed. Dover Publ., Inc., 1945.

8. Sternfeld, H.; Spencer, R. H.; and Schairer, J. O.: An Investigation of Noise Generation on a Hovering Rotor. Doc. No. D210-10229-1 (Contract DAHC04-69-C-0087), Vertol Div., Boeing Co., Jan. 1971.

9. Measurements of Aircraft Exterior Noise in the Field. ARP 796, Soc. Automot. Eng., Inc., June 15, 1965.

10. Stoffel, S. W.: NASA-Langley Helicopter Tower Instrumentation System. NASA CR-132522, 1974.

11. Spencer, R. H.: Application of Vortex Visualization Test Techniques to Rotor Noise Research. American Helicopter Soc. Preprint No. 470, June 1970.

12. Hosier, Robert N.; and Mayes, William H.: A Procedure for Predicting Internal and External Noise Fields of Blowdown Wind Tunnels. NASA TM X-2556, 1972.

13. Johnson, H. Kevin: Development of an Improved Design Tool for Predicting and Simulating Helicopter Rotor Noise. USAAMRDL-TR-74-37, U.S. Army, June 1974. (Available from DDC as AD 785 579.)

14. Johnson, H. Kevin; and Katz, Walter M.: Investigation of the Vortex Noise Produced by a Helicopter Rotor. USAAMRDL Tech. Rep. 72-2, U.S. Army, Feb. 1972. (Available from DDC as AD 741 778.)

15. Johnson, H. Kevin: Development of a Technique for Realistic Prediction and Electronic Synthesis of Helicopter Rotor Noise. USAAMRDL Tech. Rep. 73-8, U.S. Army, Mar. 1973.

TABLE I.- SUMMARY OF BLADE INSTRUMENTATION AND MICROPHONE POSITIONS

Test series	Strain-gage locations, percent span		Surface pressure transducer locations at 0.20c, percent span		Internal pressure transducers		Microphone locations		
	Blade 1	Blade 2	Blade 1	Blade 2	Blade 1	Blade 2	Distance from tower, m	Azimuth angle, deg (a)	Height off ground, m
1	29, 42, 55, 70, and 85	29	None	None	No	No	46	0, 45, 90, 135, 180, 225, 270, and 315	1.52
2	Same as test series 1	Same as test series 1	75, 85, and 95	None	Yes	Yes	76	0, 45, 90, 180, 270, and 315	0.76
							76	0	13.7
							0	On axis	18.3
3	Same as test series 1	Same as test series 1	Not applicable	Not applicable	Yes	Yes	Not applicable		
4	Same as test series 1	Same as test series 1	Not applicable	Not applicable	No	No	Not applicable		
5	Same as test series 1	Same as test series 1	85	None	No	No	Same as test series 2		

[a]The reference azimuth position (0^{o}) is upwind, and the positions are listed clockwise for an observer facing the wind.

TABLE II.- SUMMARY OF WHIRL TOWER TEST CONDITIONS

Test series	Ω, rpm	Rotor thrust, kN	Prevailing wind conditions	Smoke	Tip air mass injection conditions
1	230	8.9	N, 9 to 22 km/hr	No	No injection
	230	11.1	N, 9 to 22 km/hr		
	230	22.2	N, 9 to 22 km/hr		
	292	52.5	N, 9 to 16 km/hr		
	324	17.8	N, 9 to 22 km/hr		
	324	22.2	N, 9 to 22 km/hr		
	324	33.3	N, 9 to 22 km/hr		
	324	45.3	N, 9 to 22 km/hr		
	324	51.1	N, 9 to 22 km/hr		
2	292	21.3	N, 6 to 13 km/hr	Yes	$V_j < a$, $T_j = 71$ N, injection – both blades
	320	25.3	N, 6 to 13 km/hr		$V_j \leq a$, $T_j = 71$ and 142 N, injection – both blades
	320	27.1	N, 6 to 13 km/hr		No injection
	320	44.5	N, 6 to 13 km/hr		$V_j < a$, $T_j = 71$ and 142 N, injection – both blades
3	300	31.1	Calm	Yes	$V_j < a$, $T_j = 71$ N, injection – one blade $V_j = a$, $T_j = 142$ N, injection – both blades
4	250	26.6	Calm	Yes	$V_j = 1.5a$, $T_j = 98$ N, injection – one blade
	292	31.1			$V_j = 1.5a$, $T_j = 98$ N, injection – one blade
	324	35.5			$V_j = 1.5a$, $T_j = 98$ N, injection – one blade
5	250	26.6	NNE, 8 to 16 km/hr	No	$V_j = 1.5a$, $T_j = 98$ N, injection – one blade
	292	21.6	NNE, 6 to 10 km/hr		$V_j = 1.5a$, $T_j = 98$ N, injection – one blade
	292	31.1	NNE, 6 to 10 km/hr		$V_j = 1.5a$, $T_j = 98$ N, injection – one blade
	324	35.5	NNE, 8 to 11 km/hr		$V_j = 1.5a$, $T_j = 98$ N, injection – one blade

TABLE III.- SUMMARY OF PERFORMANCE DATA

Test series	Rotor rotational speed, rpm	Rotor thrust, kN	Rotor torque, kN-m	Jet power, kW	Jet thrust, N (a)	Jet velocity, m/sec	Rotor power, kW
2	320	45.21	20.84	---	---	---	698.0
2	320	44.48	20.12	22.4	71	317	674.1
2	320	25.93	11.14	---	---	---	372.8
2	320	25.76	10.84	22.4	71	371	363.2
5	324	36.11	14.04	---	---	---	475.8
5	324	36.17	14.08	42.5	98	433	477.2
5	324	35.88	13.96	47.7	111	433	473.5
2	292	21.96	9.39	---	---	---	287.1
2	292	21.76	9.11	22.4	71	317	278.1
5	292	21.93	8.56	---	---	---	261.7
5	292	21.39	8.14	42.5	98	433	249.1
5	292	31.30	12.59	---	---	---	384.8
5	292	31.20	12.21	42.5	98	433	372.8
5	292	31.44	11.99	47.7	111	433	366.9
5	250	11.81	4.84	---	---	---	126.8
5	250	11.95	4.38	42.5	98	433	114.8
5	250	26.75	10.53	---	---	---	275.2
5	250	26.73	10.16	42.5	98	433	266.2

[a]In test series 2, injection was applied from both blades, while in test series 5, injection was applied from one blade.

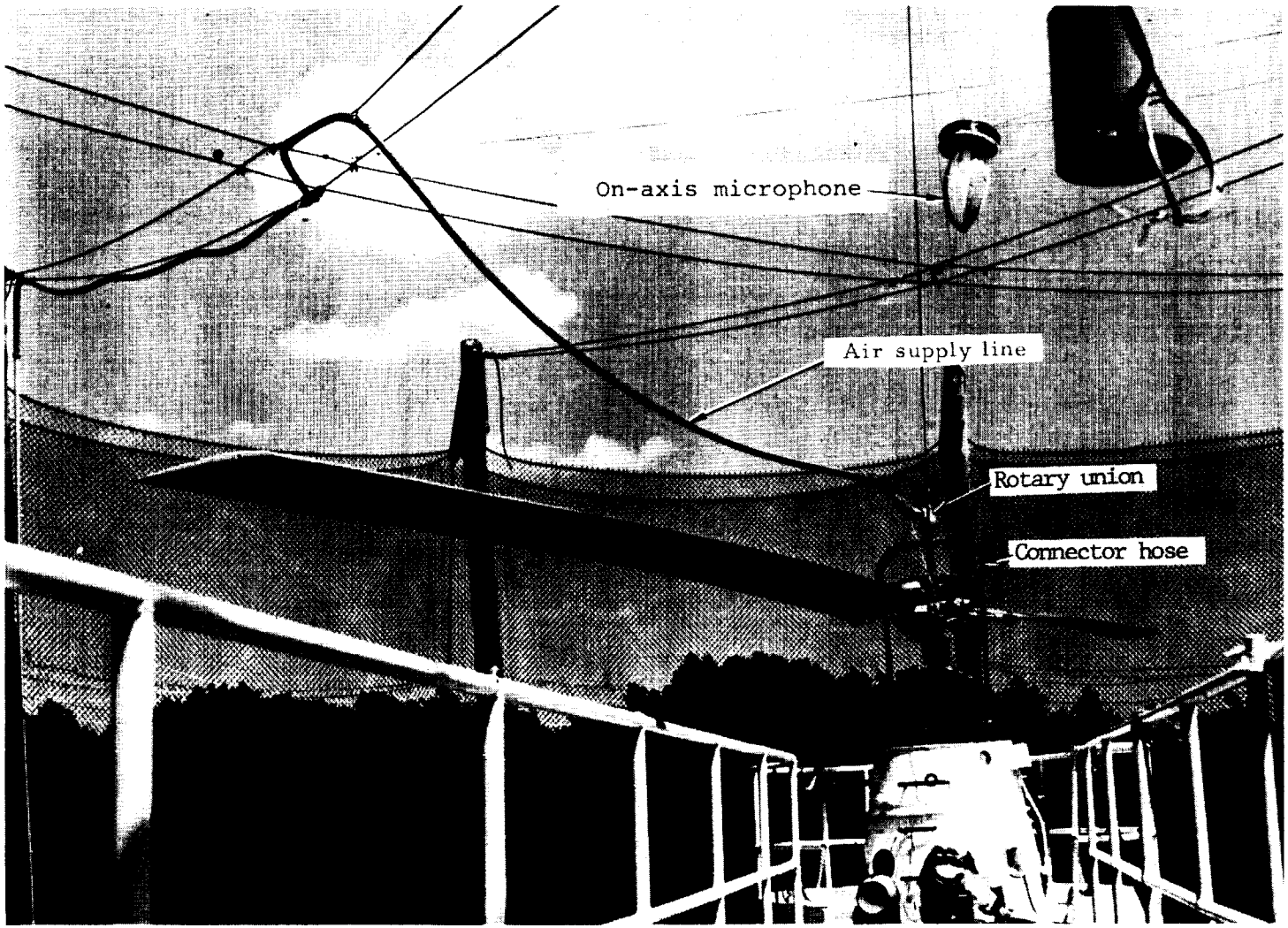

L-73-6209.1

Figure 1.- Whirl-tower installation.

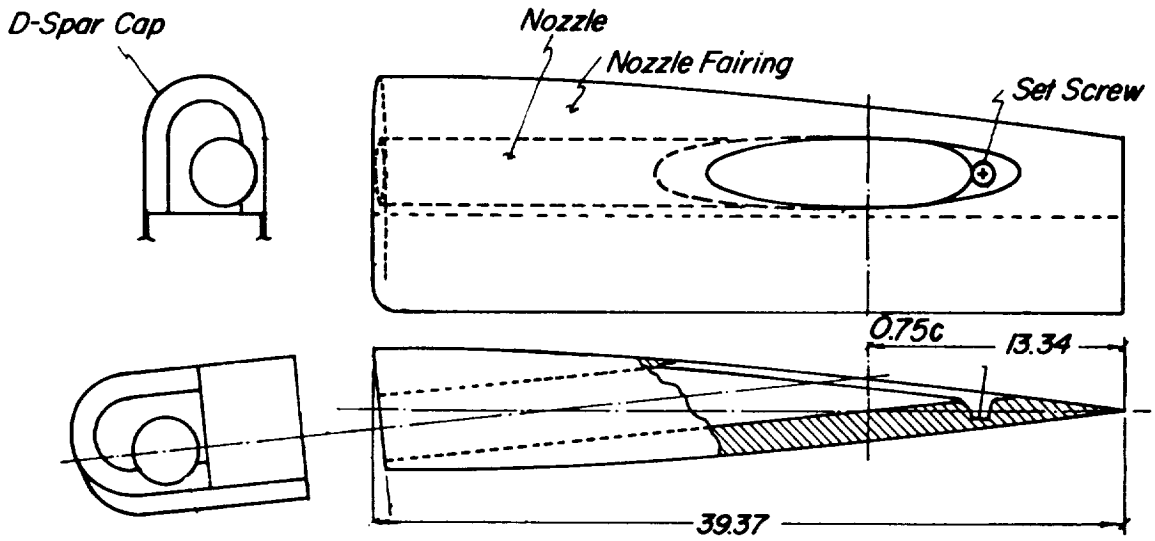

Figure 2.- Schematic of nozzle and blade tip extension (all dimensions in cm).

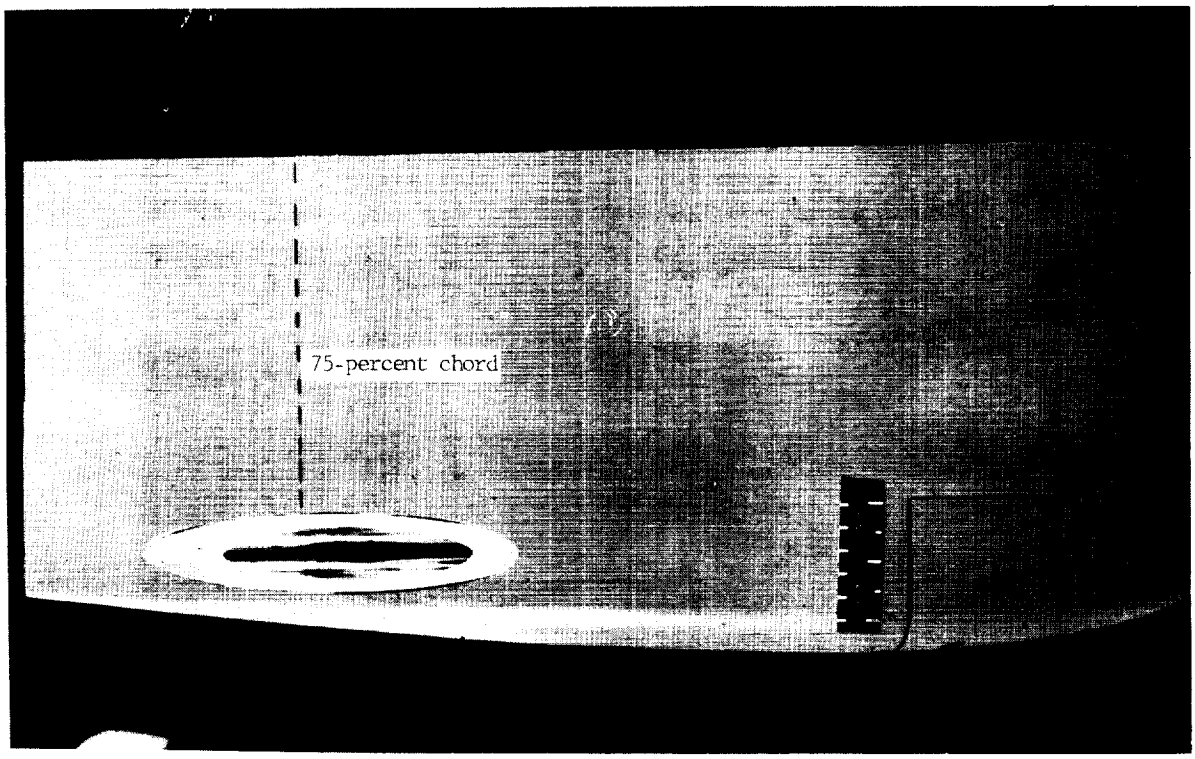

L-73-2118.1

Figure 3.- Completed tip extension installation.

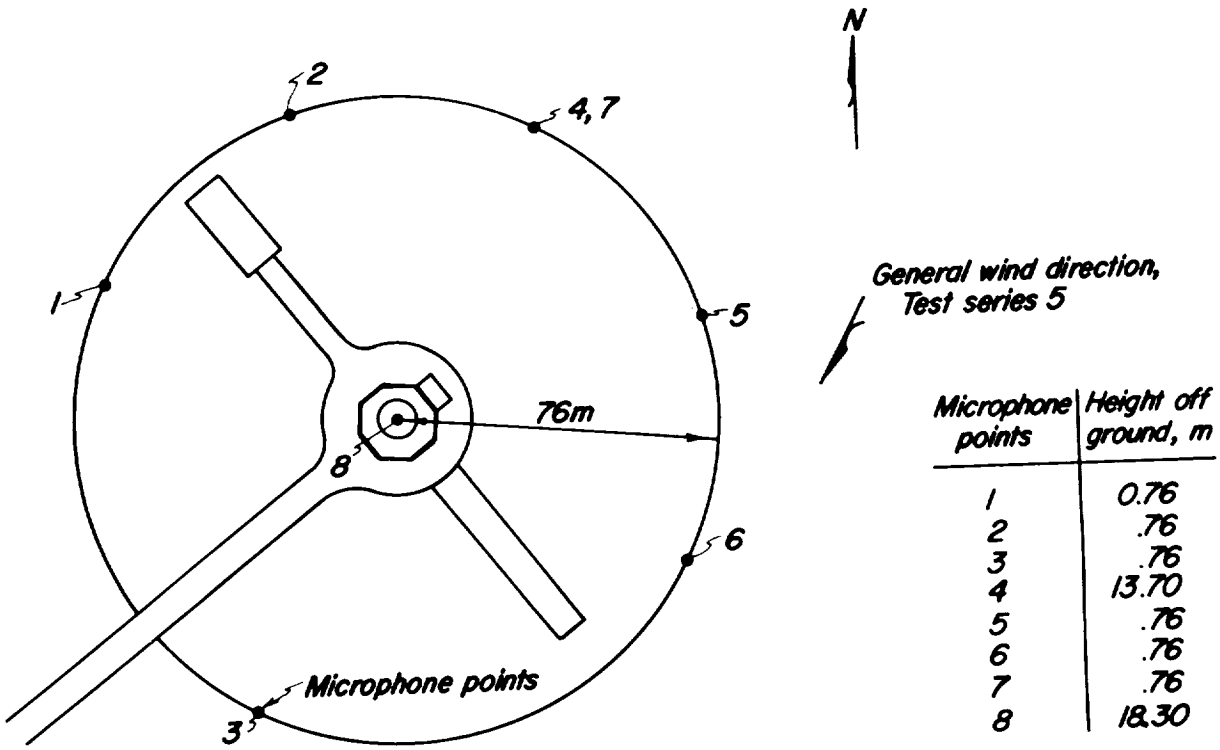

Microphone points	Height off ground, m
1	0.76
2	.76
3	.76
4	13.70
5	.76
6	.76
7	.76
8	18.30

Figure 4.- Microphone positions; test series 5.

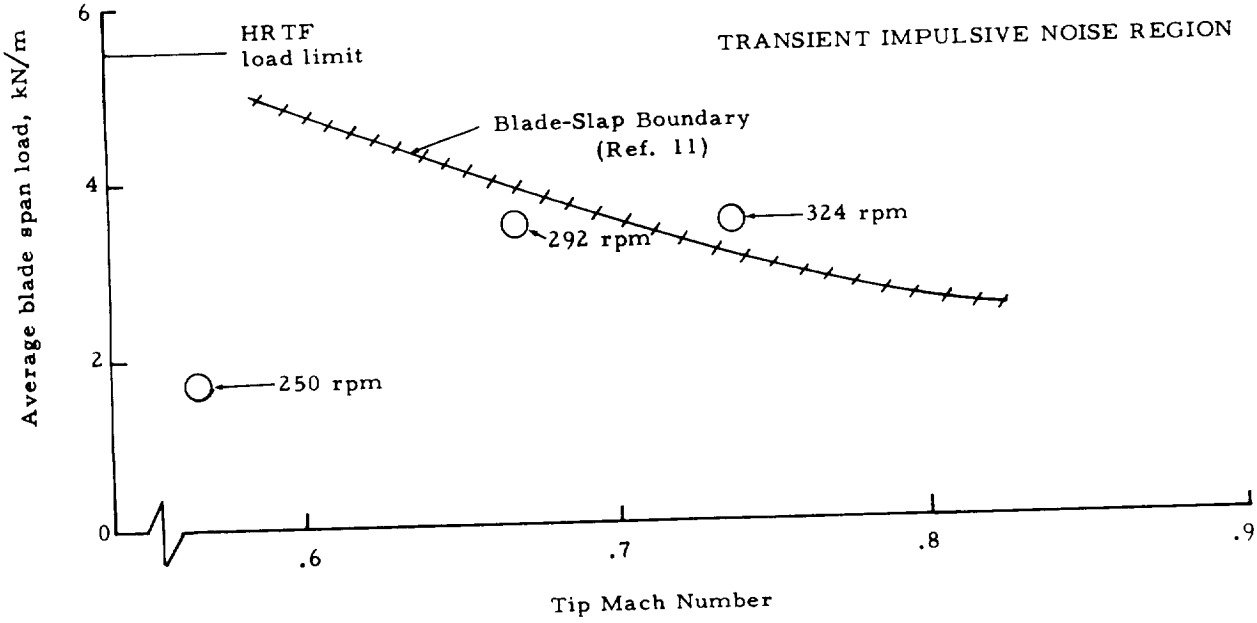

Figure 5.- Transient impulsive noise boundary in terms of average span loading

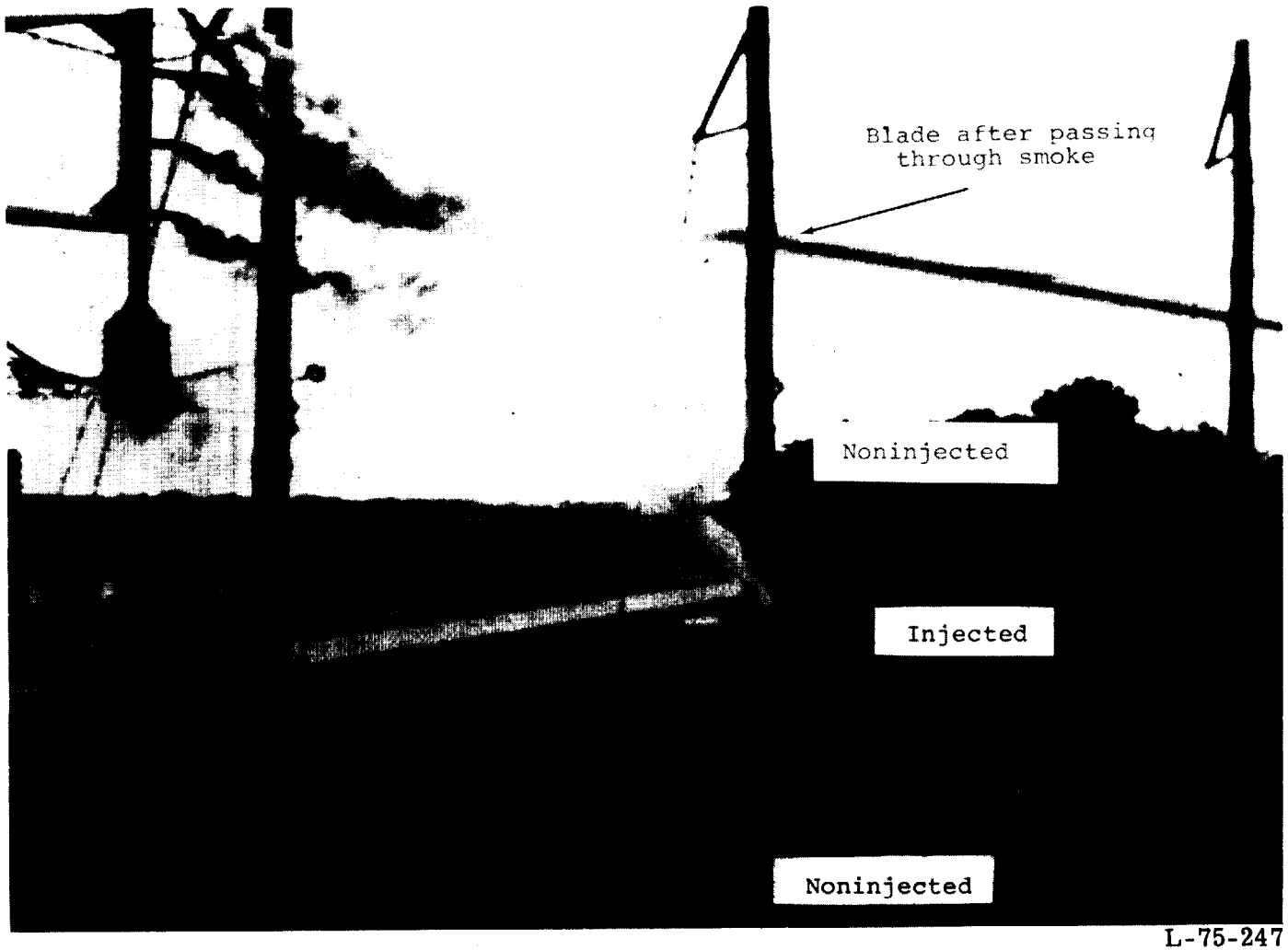

Figure 6.- Flow visualization using smoke of injected and noninjected vortices with sonic injection.

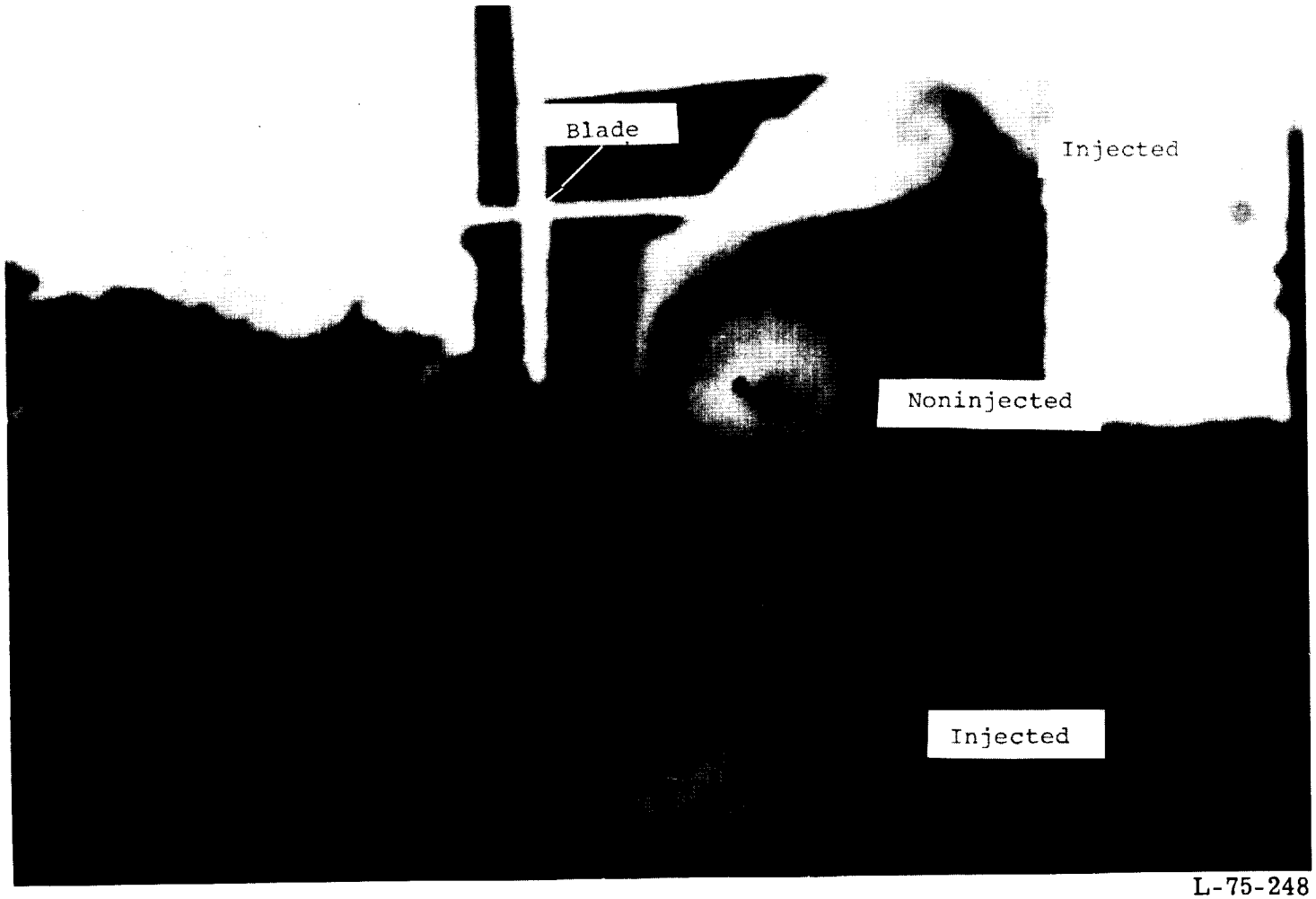

Figure 7.- Flow visualization using smoke of injected and noninjected vortices with supersonic injection.

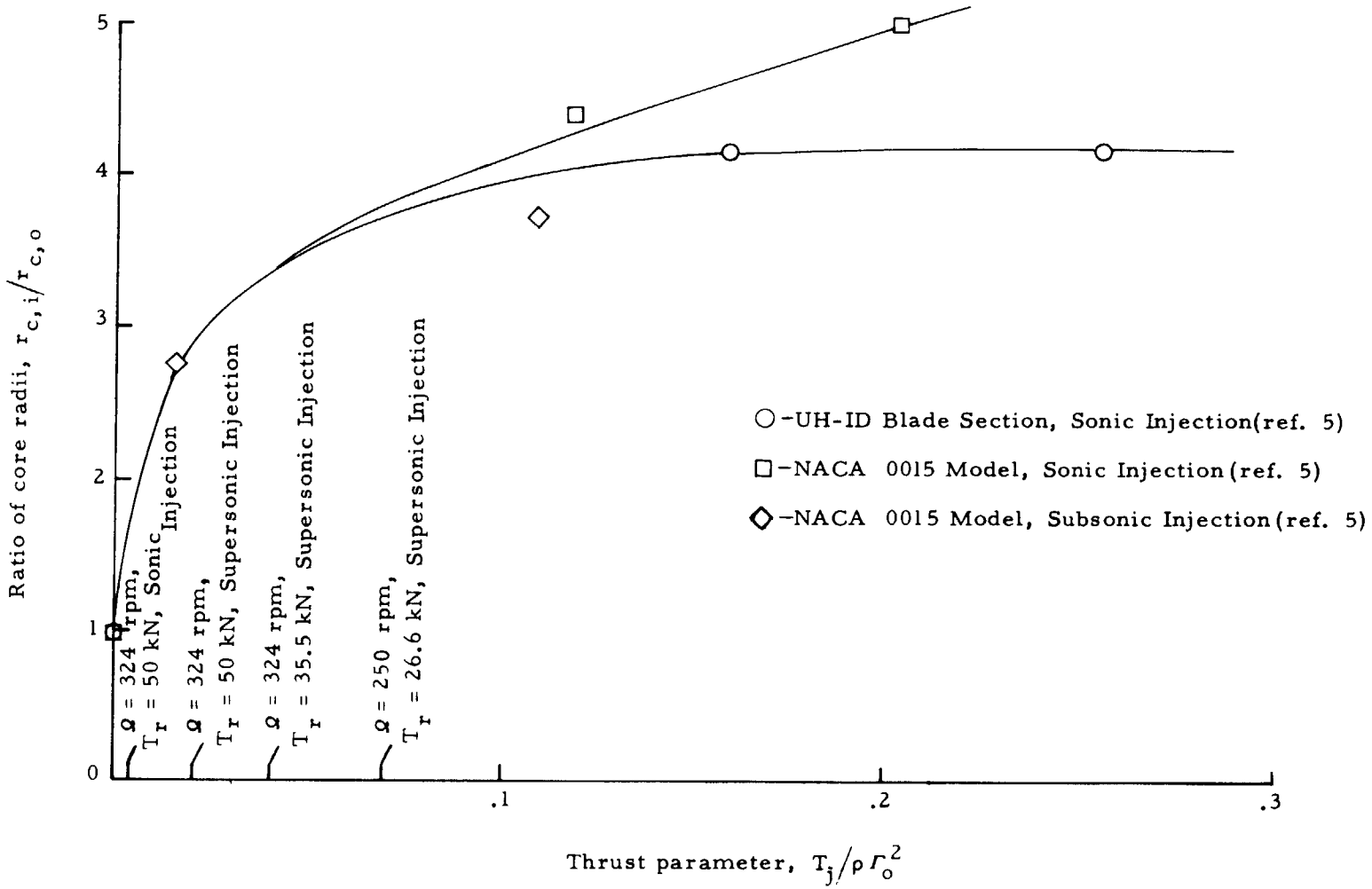

Figure 8.- Core radius of the trailing vortex for the 0.533-m- and the 0.203-m-chord semispan models at 6.5 chord lengths as a function of jet thrust. HRTF thrust parameter operating points are indicated along abscissa.

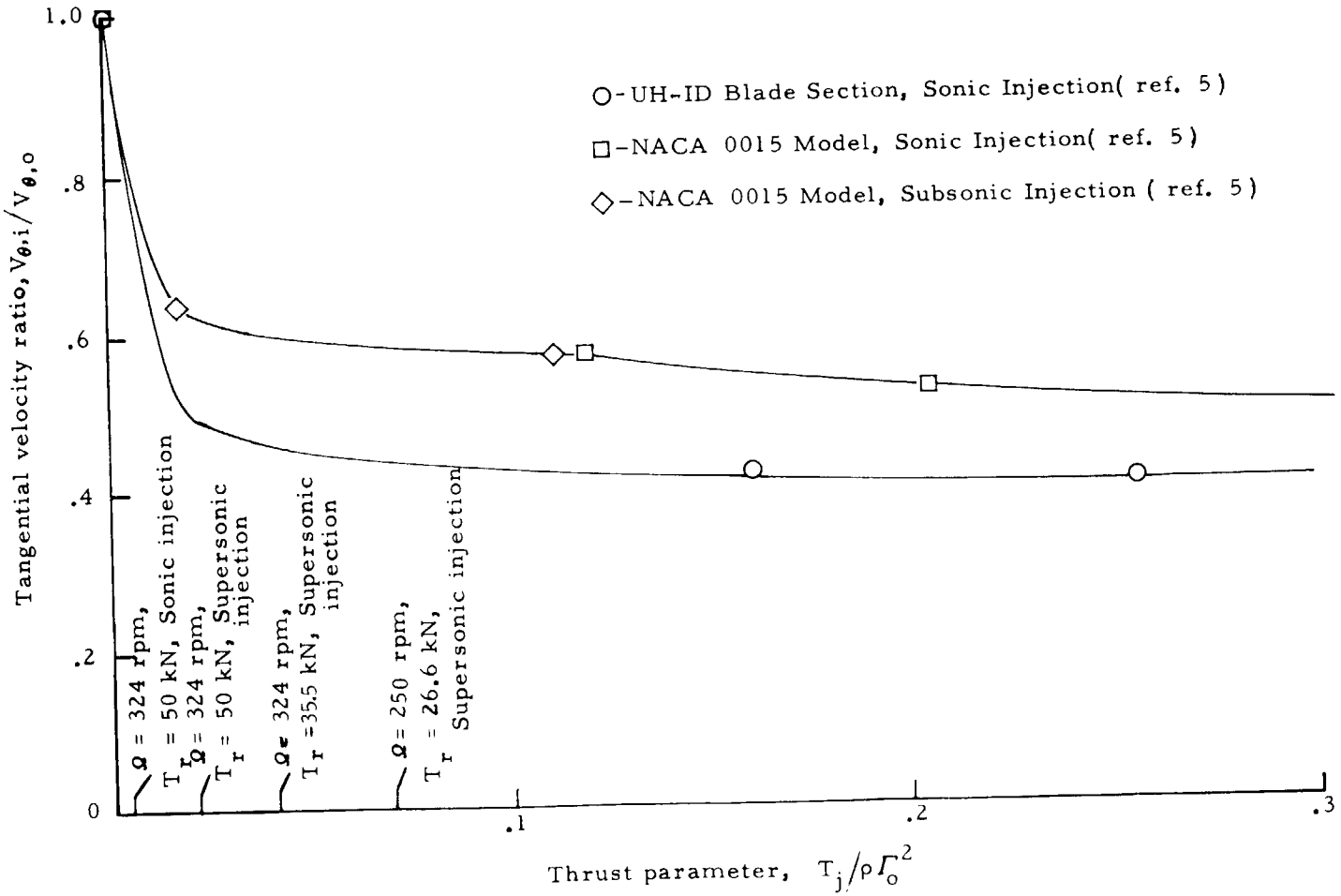

Figure 9.- Peak tangential velocity of the trailing vortex for the 0.533-m- and 0.203-m-chord semispan models at 6.5 chord lengths as a function of jet thrust. HRTF thrust parameter operating points are indicated along the abscissa.

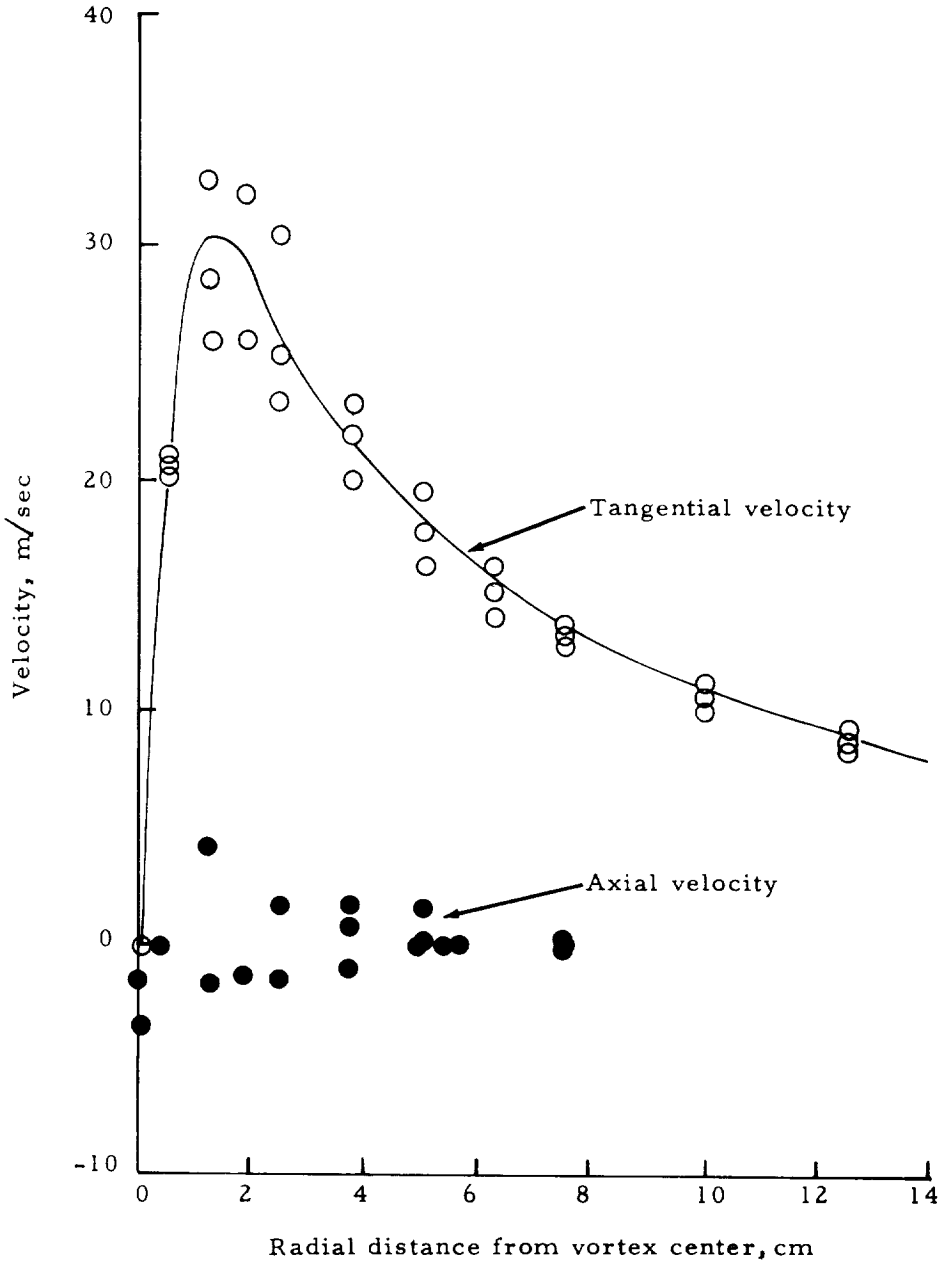

Figure 10.- Mean velocity distribution of the trailing vortex for the 0.533-m-chord model without mass injection. 6.5 chord lengths; V_∞ = 45.6 m/sec; $\alpha = 8.5^\circ$ (ref. 5).

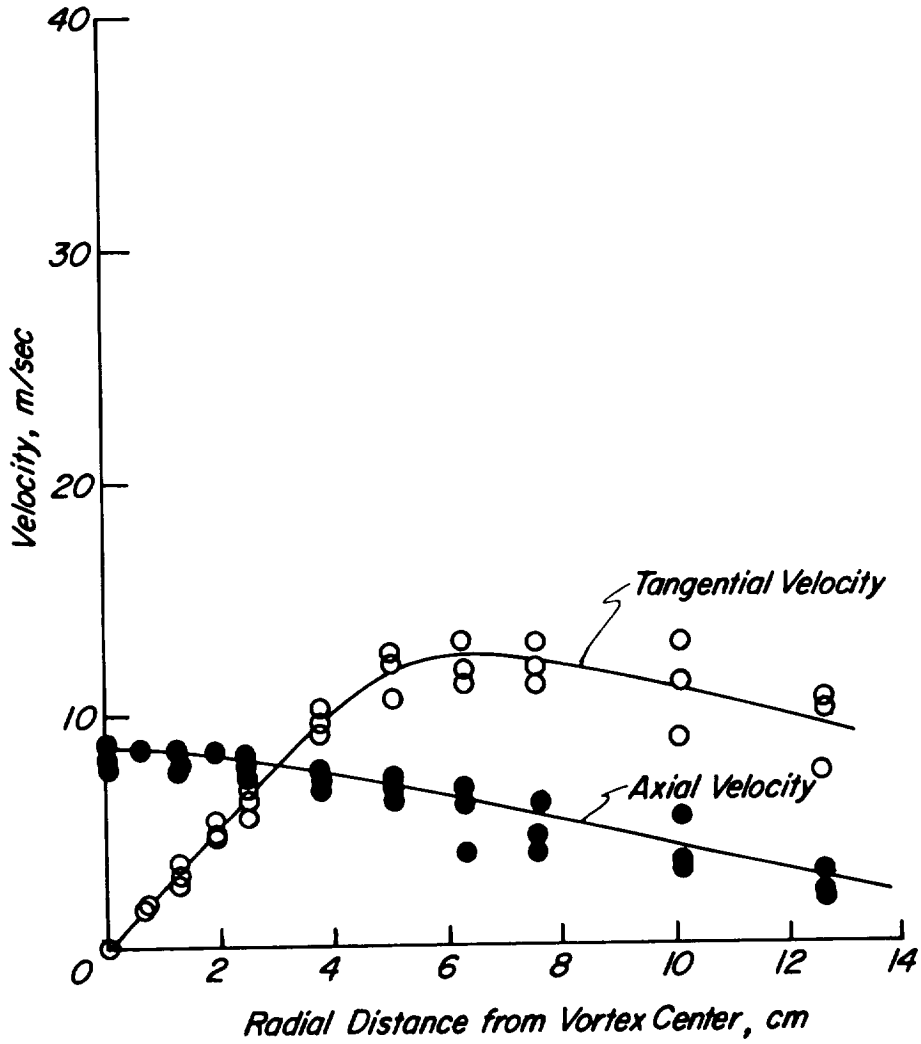

Figure 11.- Mean velocity distribution of the trailing vortex for the 0.533-m-chord model with 1.59-cm-diameter sonic nozzle. $\dot{m}$ = 0.0816 kg/sec; 6.5 chord lengths; V_∞ = 45.6 m/sec; $\alpha = 8.5^\circ$ (ref. 5).

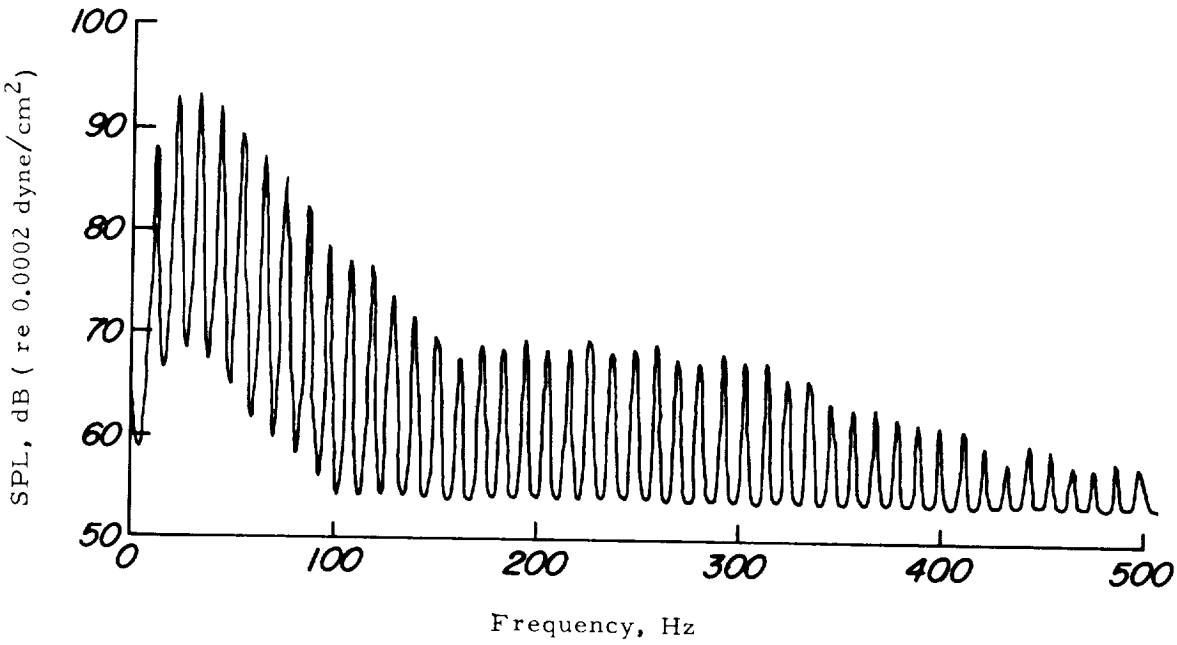

Figure 12.- Measured noise spectrum without mass injection. T_r = 35.5 kN; Ω = 324 rpm; microphone position 4; BW = 1.5 Hz.

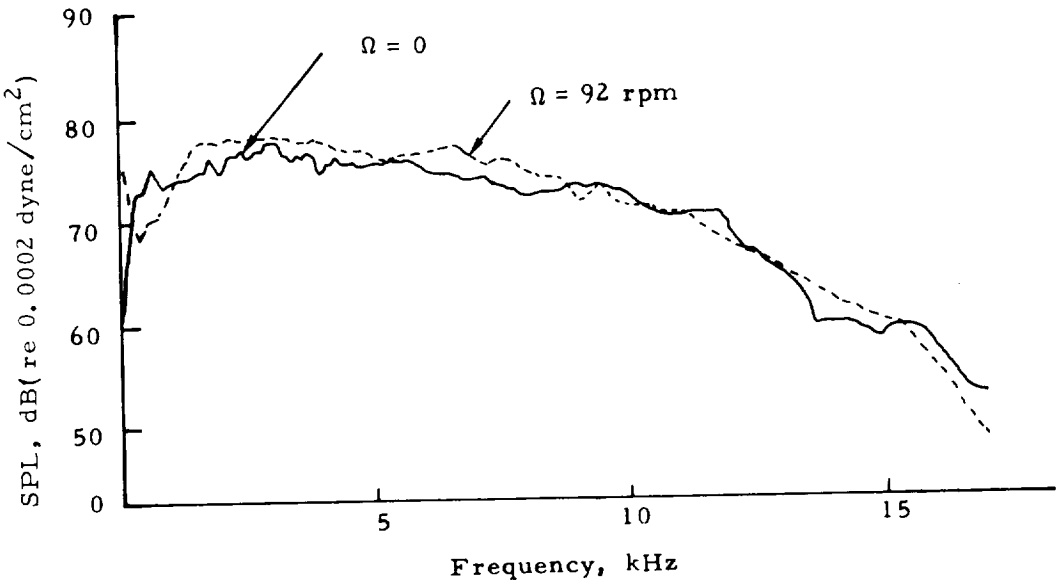

(a) Measured noise spectrum of jet TAMI; microphone position 8; $T_r = 0$; $T_j = 111$ N; BW = 60 Hz

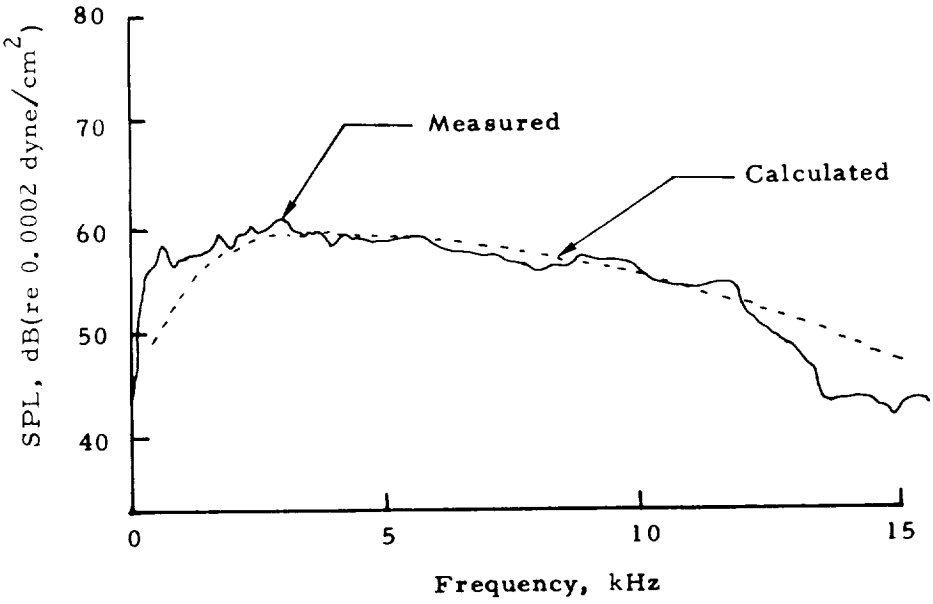

(b) Comparison of calculated and measured noise spectrum of jet TAMI; microphone position 8; $T_r = 0$; $T_j = 111$ N; $\Omega = 0$; BW = 1 Hz.

Figure 13.- Measured and calculated TAMI jet noise spectra.

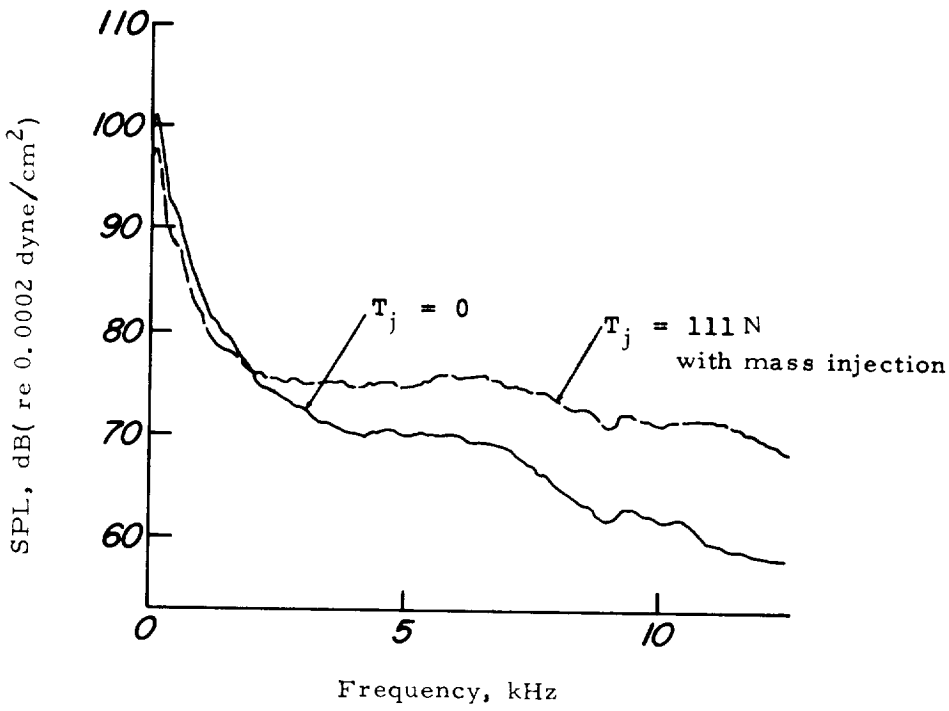

Figure 14.- Measured rotor noise spectrum with and without mass injection. T_r = 35.5 kN; Ω = 324 rpm; BW = 60 Hz; microphone position 8.

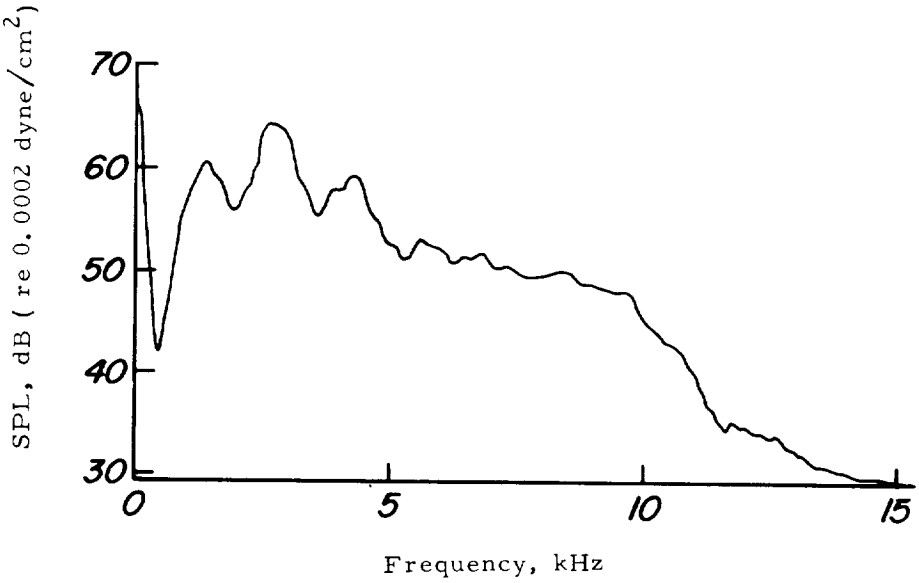

Figure 15.- Measured noise spectrum of TAMI jet. Microphone position 4; T_r = 0; T_j = 111 N; Ω = 92 rpm; BW = 60 Hz.

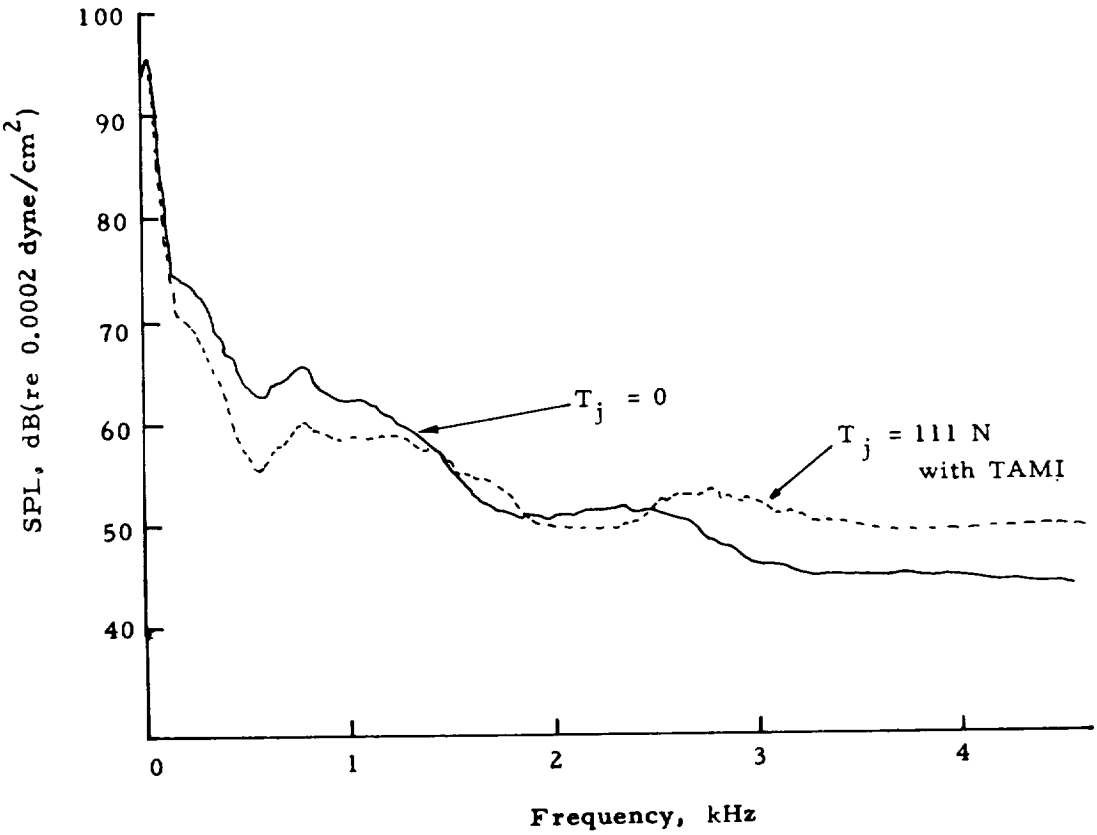

Figure 16.- Measured noise spectrum with and without mass injection. T_r = 35.5 kN; Ω = 324 rpm; microphone position 4; BW = 15 Hz.

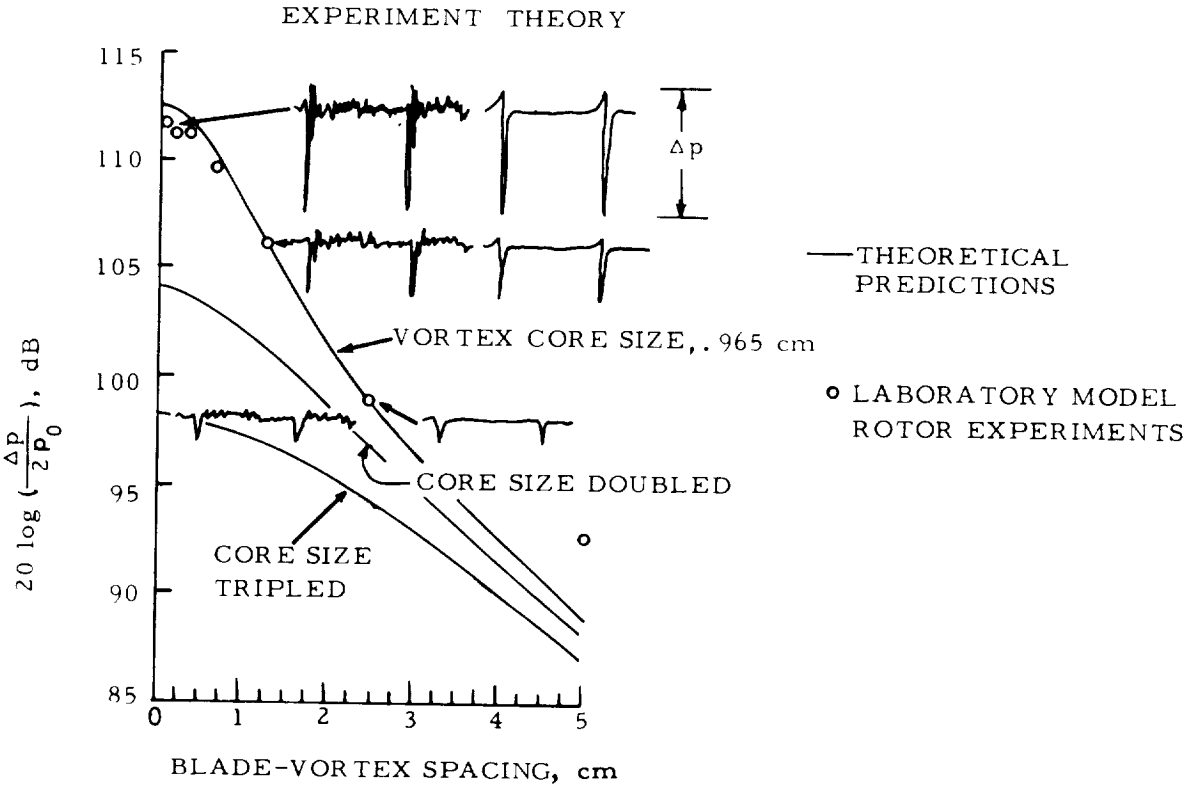

Figure 17.- The effect of blade-vortex spacing (as measured from core axis) on blade-vortex interaction noise (from ref. 1).

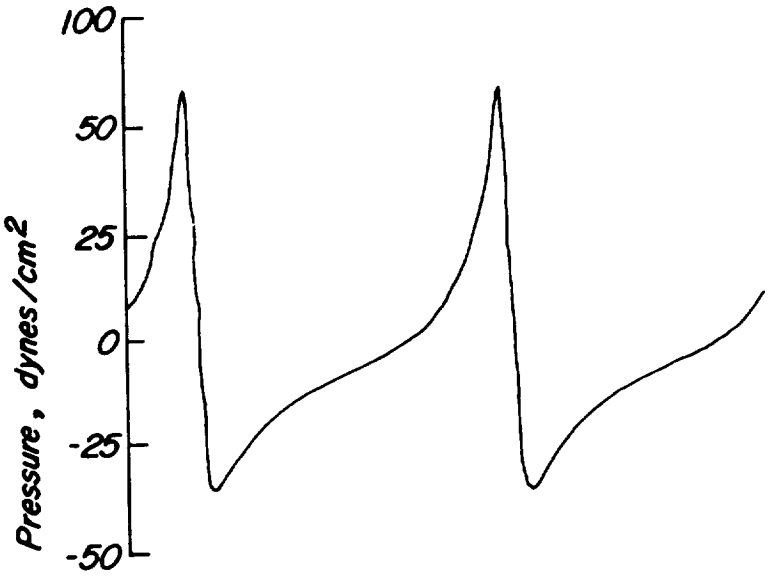

(a) Minimum vortex-rotor separation distance, 0.305 m.

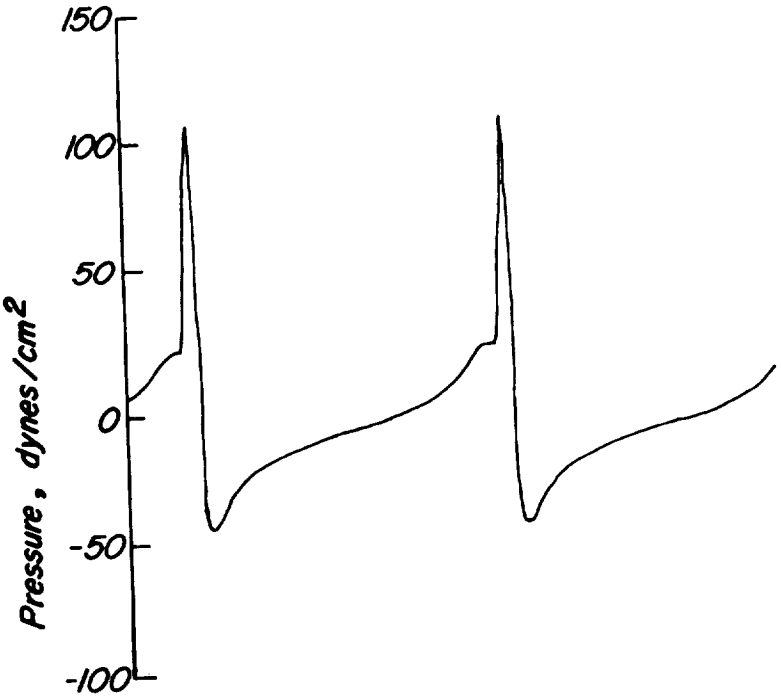

(b) Minimum vortex-rotor separation distance, 0.153 m.

Figure 18. Calculated pressure time history of rotational noise. T_r = 35.5 kN; Ω = 324 rpm; microphone position 4.

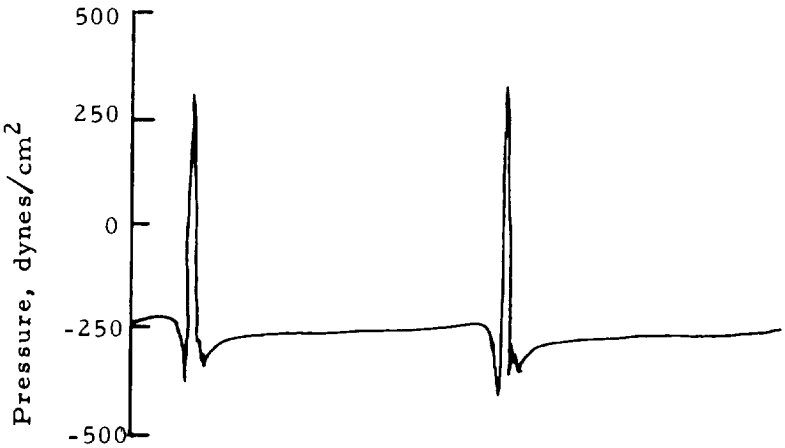

(c) Minimum vortex-rotor separation distance, 0.025 m.

Figure 18.- Concluded.

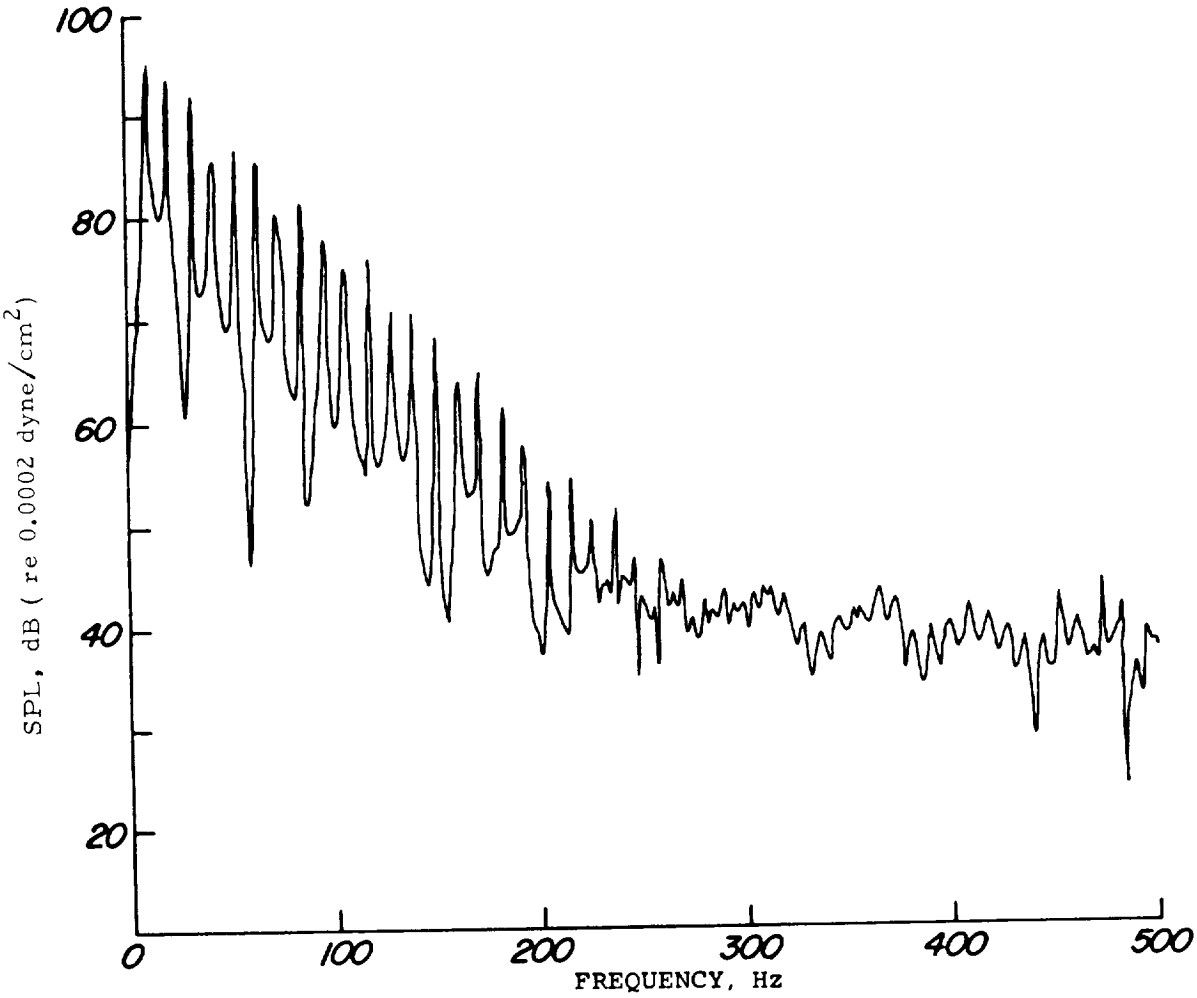

(a) Minimum vortex-rotor separation distance, 0.305 m.

Figure 19.- Calculated rotational noise spectrum. T_r = 35.5 kN; Ω = 324 rpm; microphone position 4.

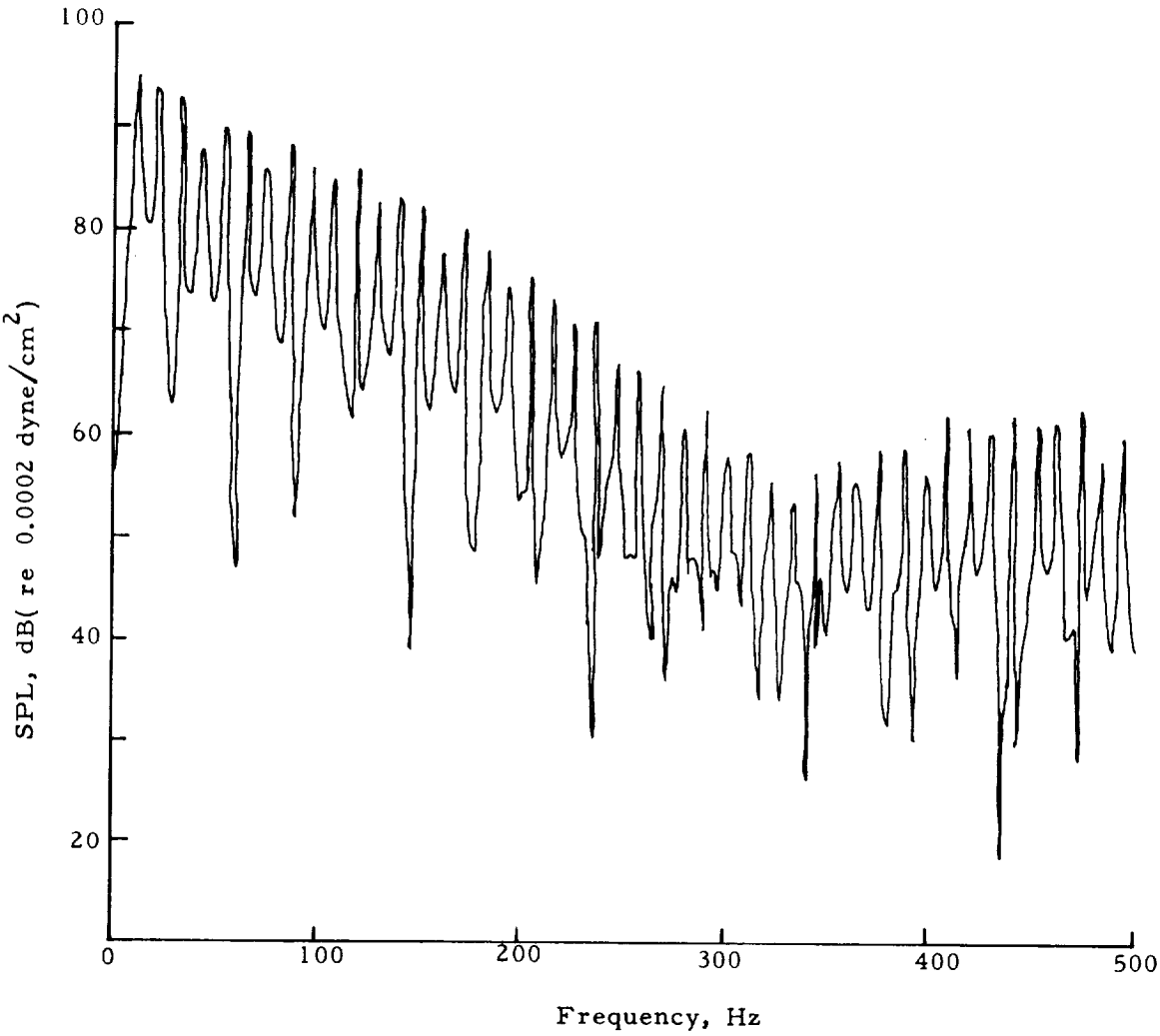

(b) Minimum vortex-rotor separation distance, 0.153 m.

Figure 19.- Continued.

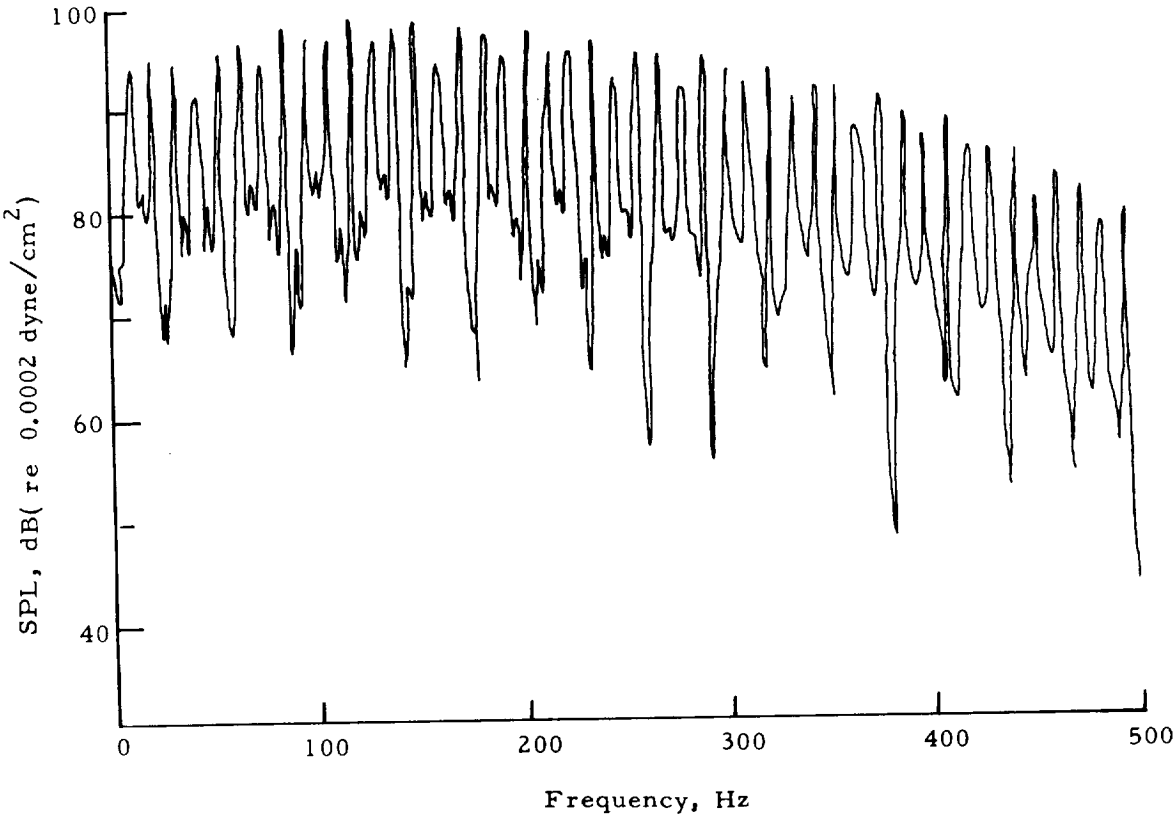

(c) Minimum vortex-rotor separation distance, 0.025 m.

Figure 19.- Concluded.

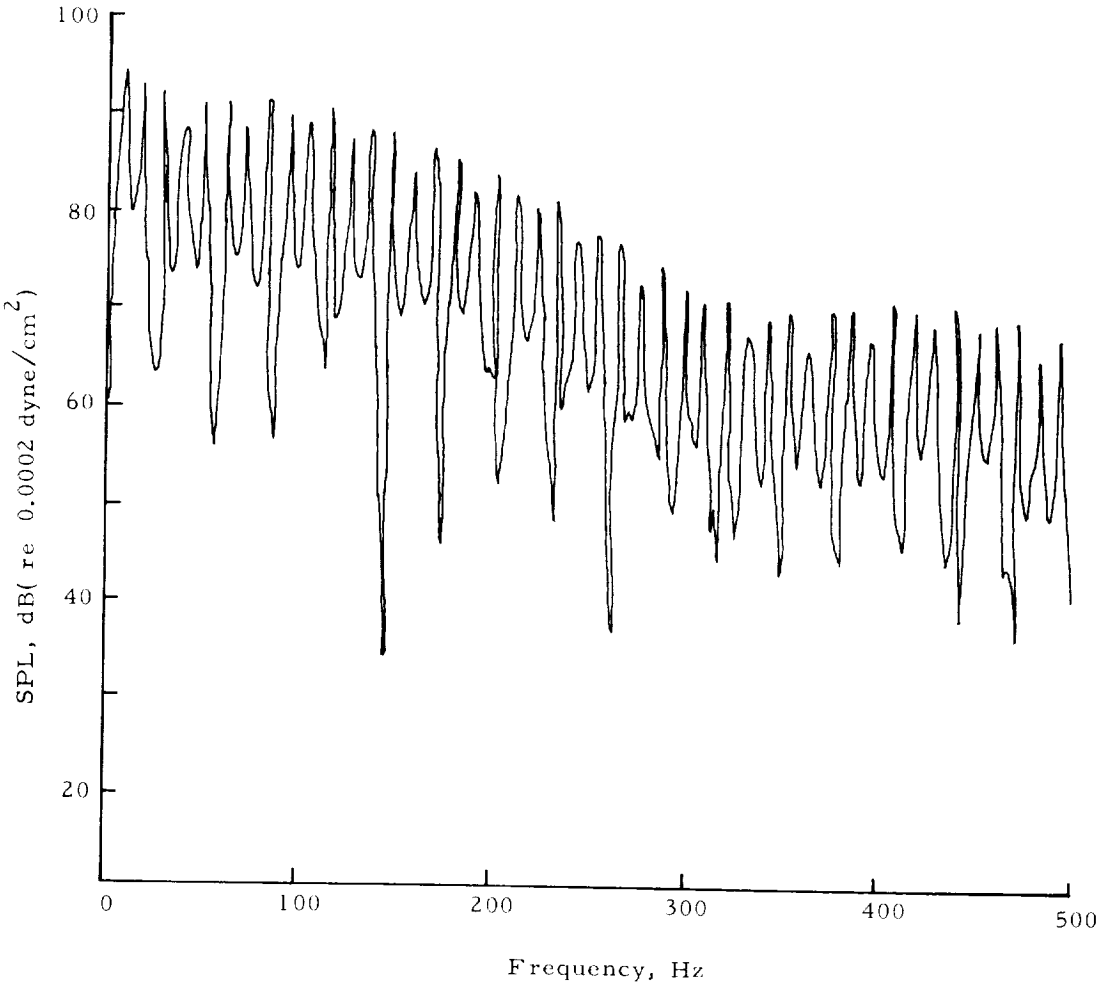

Figure 20.- Calculated rotational noise spectrum with blade-vortex interaction of mass-injected vortex. T_r = 35.5 kN; Ω = 324 rpm; minimum vortex-rotor separation distance, 0.104 m; microphone position 4.

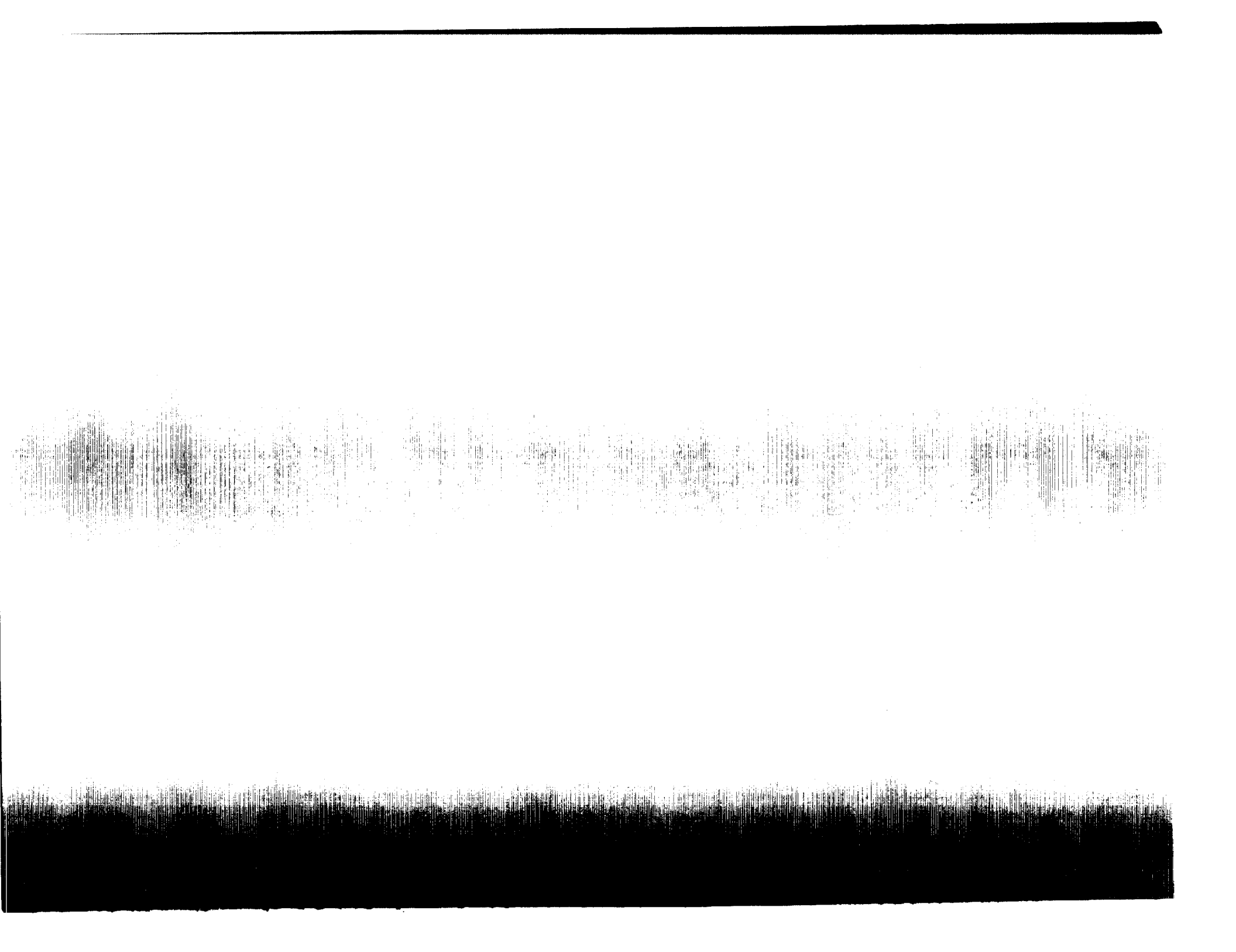

NATIONAL AERONAUTICS AND SPACE ADMINISTRATION
WASHINGTON, D.C. 20546

OFFICIAL BUSINESS
PENALTY FOR PRIVATE USE $300

SPECIAL FOURTH-CLASS RATE
BOOK

POSTAGE AND FEES PA
NATIONAL AERONAUTICS
SPACE ADMINISTRATIO
451

POSTMASTER : If Und
Postal

"The aeronautical and space activities of the United States shall be conducted so as to contribute . . . to the expansion of human knowledge of phenomena in the atmosphere and space. The Administration shall provide for the widest practicable and appropriate dissemination of information concerning its activities and the results thereof."

—NATIONAL AERONAUTICS AND SPACE ACT OF 1958

NASA SCIENTIFIC AND TECHNICAL PUBLICATI

TECHNICAL REPORTS: Scientific and technical information considered important, complete, and a lasting contribution to existing knowledge.

TECHNICAL NOTES: Information less broad in scope but nevertheless of importance as a contribution to existing knowledge.

TECHNICAL MEMORANDUMS: Information receiving limited distribution because of preliminary data, security classification, or other reasons. Also includes conference proceedings with either limited or unlimited distribution.

CONTRACTOR REPORTS: Scientific and technical information generated under a NASA contract or grant and considered an important contribution to existing knowledge.

TECHNICAL TRANSLATIONS: Inform published in a foreign language consider to merit NASA distribution in English.

SPECIAL PUBLICATIONS: Information derived from or of value to NASA activit Publications include final reports of majo projects, monographs, data compilations, handbooks, sourcebooks, and special bibliographies.

TECHNOLOGY UTILIZATION PUBLICATIONS: Information on techno used by NASA that may be of particular interest in commercial and other non-aero applications. Publications include Tech U Technology Utilization Reports and Technology Surveys.

Details on the availability of these publications may be obtained from:

SCIENTIFIC AND TECHNICAL INFORMATION OFFICE

NATIONAL AERONAUTICS AND SPACE ADMINISTRA

Washington, D.C. 20546